arXiv:1402.5653v1 [quant-ph] 23 Feb 2014

Crucial tests of macrorealist and semi-classical gravity models with freely falling mesoscopic nanospheres

Samuel Colin[*], Thomas Durt[†], Ralph Willox[‡]

Abstract: Recently, several proposals have been made to test the quantum superposition principle in the mesoscopic regime. Most of these tests consist of a careful measurement of the loss of interference due to decoherence. Here we propose to measure, instead, the spread in position of a freely falling nanosphere. As we shall show, this parameter is sensitive to various sources of decoherence (exotic and non-exotic) but also reveals an interesting interplay between self-gravity and decoherence.

1 Introduction

The quantum superposition principle has been validated at various scales of mass and distance. For instance, double slit-like interferences have been experimentally exhibited for photons, electrons, neutrons, atoms, molecules and, more recently, macro-molecules [31, 39, 21]. These experiments aim at probing the limit of validity of quantum theory and the quantum-classical boundary. Moreover, recent progress in quantum technology (in particular in quantum optomechanics [4]) nourishes the hope that it will soon be possible to scrutinize the superposition principle at the level of mesoscopic objects (e.g. nanospheres) with masses larger than 10^6 a.m.u. [2, 44, 43, 33]. Typically the experiments proposed so far consist of measuring the decay of interference exhibited by these objects and checking whether this decay can be explained solely in terms of environmental (non-exotic) decoherence sources. The realization of these experiments would make it possible, among others, to test the validity of exotic decoherence models of spontaneous localisation such as the Ghirardi-Rimini-Weber (GRW) [19], Pearle [40] and Continuous Spontaneous Localisation (CSL) [22] models (for an extensive review of these models we invite the reader to consult reference [5]). Here we propose to proceed in a slightly different manner. Instead of measuring quantum interferences exhibited by the mesoscopic object (here a solid nanosphere), we propose to let such nanospheres fall in a zero-gravity environment (e.g. a satellite) and to measure the spread of the quantum distribution in position of their centre of mass. As we shall show, this technique delivers a probe which is sensitive to decoherence, but could also possibly reveal the influence of self-gravitational effects at the level of the wave function of the centre of mass of the nanospheres (CMWF). From this point of view it constitutes a valuable investigation tool of fundamental features exhibited by quantum systems at the classical-quantum transition.

The paper is structured as follows. Firstly we describe our experimental proposal which consists of a slight modification of a recent experimental proposal aimed at testing the equivalence principle by watching the trajectories of freely falling nanospheres [33, 32]. Then we describe a new type of numerical treatment of the joint influence of decoherence and self-gravity on the temporal evolution of the CMWF. Finally we present our numerical predictions, focusing on the possibility to test the manifestation of exotic decoherence and/or self-gravity by measuring the spread of the density matrix of the centre of the mass (CMDM) of the freely falling nanospheres.

[*]Centre for Quantum Dynamics, Griffith University, 170 Kessels Road, Brisbane, QLD 4111, Australia. Department of Physics and Astronomy, Clemson University, 120-A Kinard Laboratory, Clemson, SC 29631-0978, USA. email: scolin@clemson.edu

[†]Ecole Centrale de Marseille, Institut Fresnel, Domaine Universitaire de Saint-Jérôme, Avenue Escadrille Normandie-Niémen 13397 Marseille Cedex 20, France. email: thomas.durt@centrale-marseille.fr

[‡]Graduate School of Mathematical Sciences, the University of Tokyo, 3-8-1 Komaba, Meguro-ku, 153-8914 Tokyo, Japan. email: willox@ms.u-tokyo.ac.jp

2 Experimental proposal

Freely falling nanospheres in a zero-gravity environment (a satellite) could be used for testing the superposition principle (see e.g. the experimental proposal DECIDE-DECoherence In Double-slit Experiments [33, 32], to be carried aboard the mission MAQRO-MAcroscopic Quantum ResonatOrs [33]). They are also recognized to present potential applications regarding the test of the weak equivalence principle, i.e. the universality of free fall (CASE-Comparative Acceleration Sensing Experiments [33]). In the CASE proposal, the positions of freely falling nanospheres of various masses and compositions released from an optical trap, are accurately measured by optomechanical techniques. A conventional accelerometer controls micro-propulsion thrusters of the spacecraft in order to maintain it along a quasi-inertial trajectory. Here we propose to use this device in order to measure the quantum position spread exhibited by a nanosphere after an inertial flight of long duration. In the following we take for granted that a feedback system – combining conventional accelerometers and thrusters – makes it possible to create, inside the satellite, a zero-gravity environment during periods of the order of say 10^2 to 10^3 s, along the three directions of space. The spread in position of the freely falling nanospheres can then be measured by repeatedly dropping a pair of nanospheres from two well-calibrated positions inside optical traps, leaving them to "float" during a certain time inside the satellite. After this time it is possible to measure, with high accuracy, their position by accelerating the satellite for a while by means of its thrusters, along a direction orthogonal to a support where the spheres will remain trapped (for instance by gluing them as has been done, some years ago [31], in interference experiments involving macromolecules). By repeatedly measuring the relative positions of nanospheres of same mass and composition, we can estimate the spread of their relative position. Using two spheres, rather than one, allows us to get rid of the intrinsic uncertainty of the inertial sensor that is used for controlling the thrusters.

We shall from now on assume that the constraints which are required for the feasibility of the aforementioned DECIDE interference experiment [33, 32] (which are, among others, flights of duration of 200 s and precision in position of the order of 5 nm, low temperature and extreme vacuum conditions) are achievable experimentally (the way to complete these requirements is discussed in [33, 32]). As we shall show, these requirements guarantee suffcient accuracy to discriminate with high sensitivity exotic from non-exotic sources of decoherence and to measure the influence of self-gravity as well. They even make it possible, as we shall show, to discriminate "weak" exotic sources of decoherence which are out of reach of interference experiments. Our requirements are compatible with the reported precision on the localisation of nanospheres inside optical traps [44] (0.1 Å for nanospheres of 100 nm) and with the reported accuracy of sub-wavelength detection techniques that were developed for instance in biophotonics [34]. Similar to other high sensitivity tests of quantum theory in the mesoscopic domain, our experiments necessitate a clean environment (low gas pressure and low temperatures). This is because in normal terrestrial conditions of pressure and temperature, the environmental (non-exotic) decoherence is so important that it would mask the tiny effects that we wish to measure, be they the result of self-gravity and/or exotic decoherence. These conditions are not easy to meet at the level of a satellite but achieving them is not an impossible task. For instance, the main technological challenges for DECIDE are, among others, a pressure of 10^{-13} Pa, a nanosphere temperature T_i of 20 K and an environmental temperature of 16 K [32].

3 Exotic versus non-exotic sources of decoherence

Decoherence is omnipresent at the quantum level and, unless it is possible to isolate a system from its direct environment, the influence of decoherence is huge and very rapid [27, 47]. By non-exotic decoherence we refer to the well-documented sources of decoherence that are due to the interaction of a system with its direct physical environment. This includes scattering (by the quantum system under investigation, here a nanosphere) of residual gas particles, of thermal photons of the environment, emission and/or absorption of thermal photons and so on. By 'exotic decoherence' we wish to refer to a hypothetical mechanism of spontaneous localisation (SL) which would be active everywhere in our universe and would ultimately explain why classical objects are characterized by an unambiguous localisation in space [5]. The importance of SL models (also called macrorealist models) lies in the fact that they bring an answer to the measurement problem [6]. The GRW model [19] predicts for instance

that the quantum superposition principle is violated in such a way that a macroscopic superposition (Schrödinger cat state) will collapse into a well-resolved localised wave packet (of an extent of the order of 10^{-7} m) after a time proportional to the mass of the pointer. This time becomes very small in the classical limit, seen here as the large mass limit. For instance, the original GRW model predicts that the collapse time is of the order of 10^{-7} s for a pointer of mass equal to 10^{23} a.m.u.. There exists an extended zoology of SL models, such as those attributing the source of spontaneous localization to a dedicated universal localization mechanism (GRW [19], CSL [40, 22], Quantum Mechanics with Universal Position Localization (QMUPL) [5, 13] and Adler's SL models [1]), to self-gravitation (Diosi [13] and Penrose [41]), to fluctuations of the spacetime metric (Karolyhazy, Frenkel *et al.* [18]), or to quantum gravity (Ellis *et al.* [15, 16]) and so on. It is not our goal to give a survey of all these models here, and we invite the interested reader to consult the recent and very exhaustive review paper of Bassi *et al.* [5] dedicated to this topic as well as reference [42] where a careful estimate of the SL parameters assigned to these various models is provided. However, what these models have in common is that they all lead to accurate predictions regarding the quantum-classical transition. Here we shall consider four of them in detail, the original GRW model, the CSL model, the Diosi Penrose model (DP) and the Quantum Gravity (QG) model. Typically, in these models, a nanosphere of normal density will cross the quantum-classical transition when its radius becomes larger than 10^{-7} m. Of course the transition is not assumed to be sharp and in the rest of the paper we will study a range of radii from 10^{-8} to 10^{-5} m.

4 Self-gravitation

Although various manifestations of gravity at the macroscopic and cosmological scales have been accurately studied, it is not clear yet how gravitation is generated by a quantum object, and it is even less clear how the object interacts with itself under the influence of gravitation. Here we shall assume that in first approximation the source of gravity of a quantum object is equivalent to a classical matter density equal to $M|\Psi(t,\mathbf{x}')|^2$, where Ψ represents the CMWF of the object and M its mass. Whenever we can suppose that the object is point-like (that is, when the spread of the CMWF is much larger than the size of the object), quantum effects due to self-gravitation are encapsulated in the Schrödinger-Newton equation [11]

$$i\hbar\frac{\partial\Psi(t,\mathbf{x})}{\partial t} = -\hbar^2\frac{\Delta\Psi(t,\mathbf{x})}{2M} + \int d^3x'|\Psi(t,\mathbf{x}')|^2V(|\mathbf{x}-\mathbf{x}'|)\Psi(t,\mathbf{x}), \tag{1}$$

where $V(d) = -GM^2/d$, which can be derived from the mean field coupling limit proposed by Møller [38] and Rosenfeld [45] in the non-relativistic limit [24]. If the object possesses an internal structure, the situation is more complicated [10] and it is then necessary to integrate the self-gravitational Newtonian interaction over the degrees of freedom assigned to its internal structure. In the case of a rigid homogeneous nanosphere, this can be done exactly and one finds that, at short distance, instead of the Newton potential V, the effective self-interaction can be expressed[1] in terms of $d = |\mathbf{x}_{CM} - \mathbf{x}'_{CM}|$ as follows:

$$V^{\text{eff}}(d) = \frac{GM^2}{R}\left(-\frac{6}{5} + \frac{1}{2}\left(\frac{d}{R}\right)^2 - \frac{3}{16}\left(\frac{d}{R}\right)^3 + \frac{1}{160}\left(\frac{d}{R}\right)^5\right) \quad (d \leq 2R), \tag{2}$$

where R is the radius of the nanosphere. This expression is valid when d is smaller than twice the radius of the sphere. Otherwise, when d is larger than twice the radius of the sphere, the integration is straightforward: making use of Gauss's theorem we recover the usual Coulomb-like shape,

$$V^{\text{eff}}(d) = -\frac{GM^2}{d} \quad (d \geq 2R). \tag{3}$$

[1] There are quite a number of papers in which the authors purport to calculate this potential. Unfortunately, most of these results are incorrect. To the best of our knowledge, the only paper to give the correct expression for the Coulombian self-interaction of a homogeneously charged sphere (which is the same as the Newtonian self-interaction potential, up to a negative constant factor) is [29], where it is given without proof. Expression (2) was obtained independently, by direct calculation, by the present authors.

It should be noted that the fifth degree polynomial (in $\frac{d}{R}$) (2) agrees, up to its 4th derivative, with the Newtonian potential in $1/r$ at the transition point ($d = 2R$).

The resulting integro-differential evolution law of the CMWF now reads

$$i\hbar\frac{\partial\Psi(t,\mathbf{x_{CM}})}{\partial t} = -\hbar^2\frac{\Delta\Psi(t,\mathbf{x_{CM}})}{2M} + \int d^3x'_{CM}|\Psi(t,\mathbf{x'_{CM}})|^2 V^{\text{eff}}(|\mathbf{x}_{CM} - \mathbf{x}'_{CM}|)\Psi(t,\mathbf{x_{CM}}), \qquad (4)$$

where $V^{\text{eff}}(|\mathbf{x}_{CM} - \mathbf{x}'_{CM}|)$ is fully defined through equations (2,3).

Although self-gravitation has been invoked as a source of spontaneous localization by several authors among which Diósi and Penrose [12, 13, 41], it is not always easy from the literature on this subject to understand by which mechanism gravitational self-collapse would ultimately lead to spontaneous localization [20]. As we explain in [10], self-gravitation, *as defined through equations (2,3,4)*, does not require any extra ingredient to explain why objects localize. In our view, and this is for instance confirmed by the accurate numerical simulations carried out by van Meter [51], the non-linearity of the NS equation suffices to explain how and why quantum systems spontaneously tend to reach a stable minimal energy state in which dispersion is exactly compensated by self-gravity. From this point of view our approach differs radically from stochastic spontaneous models of self-localisation in the sense that, as was noted in [5], the Schrödinger-Newton dynamics is deterministic while quantum jumps are intrinsically stochastic. In the rest of the paper we shall thus distinguish self-gravitation *as defined through equations (2,3,4)*, from the aforementioned sources of exotic decoherence and in particular from the DP model [12, 13, 41, 42] which will be treated on the same footing as other SL models, independent from what we call self-gravitation. In any case, our study shows that at the mesoscopic scale (nanospheres with radii in the nanometer-millimeter range) the self-gravitational interaction, if it exists, cannot always be neglected. As we shall show, for a well-chosen range of parameters, decoherence and self-gravitation have comparable effects. Moreover, self-gravitation is to some extent robust with respect to decoherence. This justifies, in our opinion, the interest of studying the interplay between both phenomena.

5 Interplay between the free Schrödinger evolution, decoherence and self-gravitation

5.1 Interplay between the free Schrödinger evolution and self-gravitation

The interplay between the free Schrödinger evolution and self-gravitation has motivated an abundant literature. In particular, a lot of attention has been devoted to the properties of the ground state of the S-N equation (1), as it constitutes a natural candidate for a self-collapsed localized state [7, 8, 9, 28, 35, 48, 49]. In the literature, one also finds several attempts to (numerically) study the temporal evolution of the self-localization process that results from gravitational self-focusing [3, 46, 14, 28, 25, 26, 23, 51]. For instance, in [23] scaling arguments are combined with numerical estimates to give a lower bound of 10^{10} atomic units for the mass of an initial gaussian wave packet (with a typical width of 0.5 μm) for it to undergo collapse to the ground state.

These works are often characterized by a high level of computational complexity. The main reason is that the modified Schrödinger evolution (1) (or (2–4) depending on the physical details of the system one wishes to study) which incorporates self-gravitational interaction at the quantum level, is at the same time non-linear and non-local. This severely complicates its resolution by standard numerical methods. Another problem is that, so far, only two extreme regimes have been studied: the so-called "single particle" [36, 23] and "macroscopic" [11] regimes , which, respectively, correspond to the cases where the extent of the CMWF is considerably larger ($d \gg R$) or much smaller ($d \ll R$) than the radius of the nanosphere (in the first case, the internal structure of the sphere plays no role, and it can be considered as an object without dimension, like an electron; on the contrary, in the opposite regime, the center of mass is sharply localized and behaves as a classical point-like particle). In the experiments proposed by us however, it is necessary to also investigate the "mesoscopic" regime where the extent of the CMWF is comparable to the radius of the nanosphere ($d \approx R$). In order

to overcome these computational difficulties, we developed an approximative resolution scheme [10] which we outline below.

Essentially, we approximate the effect of self-gravitation by a harmonic potential, the spring constant of which depends non-linearly on the spread of the CMWF. The approximated evolution then reads

$$i\hbar\frac{\partial\Psi(t,\mathbf{x})}{\partial t} = -\hbar^2\frac{\Delta\Psi(t,\mathbf{x})}{2M} + \frac{k(<r^2>)}{2}r^2\Psi(t,\mathbf{x}), \tag{5}$$

where $k(<r^2>)$ is a function of $<r^2>=\int d^3x\left|\psi(\mathbf{x},t)\right|^2 r^2$, which remains to be defined. This equation is not linear, unless k is a constant function (as occurs in the macroscopic regime), but it possesses appealing properties which are in fact very close to those of the modified Schrödinger evolutions (1) (or (2–4) in the general case) we wish to study:

(i) if initially the CMWF is gaussian, it will remain so at all times. In particular, if we impose a gaussian ansatz for the solution of the form $\Psi(t,\mathbf{x})$=exp$(-Ar^2 + B_x x + B_y y + B_z z + C)$, we obtain a closed system of differential equations for the complex functions of time $A(t)$, $B_x(t)$, $B_y(t)$, $B_z(t)$, $C(t)$. The evolution law of $A(t)$ is particularly simple:

$$\frac{dA(t)}{dt} = \frac{-2i\hbar A^2}{M} + \frac{ik(<r^2>)}{2\hbar}, \tag{6}$$

where $<r^2>=3/(4Re(A))$. In fact, this leads to a substantial gain in computational time.

It is worth noting that although the effective potential (2,3) is translationally invariant, this is not the case for the harmonic potential in equation (5). However, because of the Galilean invariance of the gravitational self-interaction, one can associate equation (5) with the self-interaction expressed in a co-moving referential, with origin at the center of the CMWF (and for which $<r>=0$), thereby effectively enforcing translational invariance in the approximation. The main effect of self-gravitation will therefore manifest itself at the level of the spread $<r^2>$ of the CMWF (or the density matrix of the center-of-mass wavefunction (CMDM) in the case of a Monte Carlo approach *à la* GRW, as we shall see later on) which is precisely the quantity that we want to address experimentally.

(ii) it possesses a conserved quantity $E^{\rm cons}$, similar to an energy which reads

$$E^{\rm cons} = \frac{\hbar^2}{2M}\int d^3x\ \left(\left|\nabla\psi(\mathbf{x},t)\right|^2 + \left|\psi(\mathbf{x},t)\right|^2 V^{cons}(<r^2>)\right) \tag{7}$$

where the conserved potential is obtained after integrating the function k:

$$\frac{dV^{cons}(<r^2>)}{d<r^2>} = \frac{k(<r^2>)}{2}. \tag{8}$$

In general, identifying the conserved potential with the effective potential (2,3), that is, imposing $V^{cons}(<r^2>) = V^{eff}(d=\sqrt{<r^2>})$ unambiguously defines the spring constant k:

$$k(<r^2>) = (GM^2/R^3)(1-(9/16)\tilde{d}+(1/32)\tilde{d}^3) \tag{9}$$

with $\tilde{d}=\sqrt{<r^2>}/R$ when $\sqrt{<r^2>}\leq 2R$, and

$$k(<r^2>) = \frac{GM^2}{(\sqrt{<r^2>})^3} \tag{10}$$

when $\sqrt{<r^2>} > 2R$.

It is worth noting that the spring constant and its first three derivatives remain continuous at the transition point $\sqrt{<r^2>}=2R$. As is discussed in detail in another paper of ours [10], in the region $\sqrt{<r^2>}\ll 2R$ (the macroscopic regime) our approximation is in fact exact if we consider states which obey our gaussian ansatz because in that region the effective potential is indeed harmonic, as was pointed out by Diosi [11], and the effective evolution (4) is therefore also harmonic. The nature of our approximation (5,10) in the single particle regime is best understood in the following way: in a sense it amounts to replacing the self-gravitational potential generated by a CMWF of

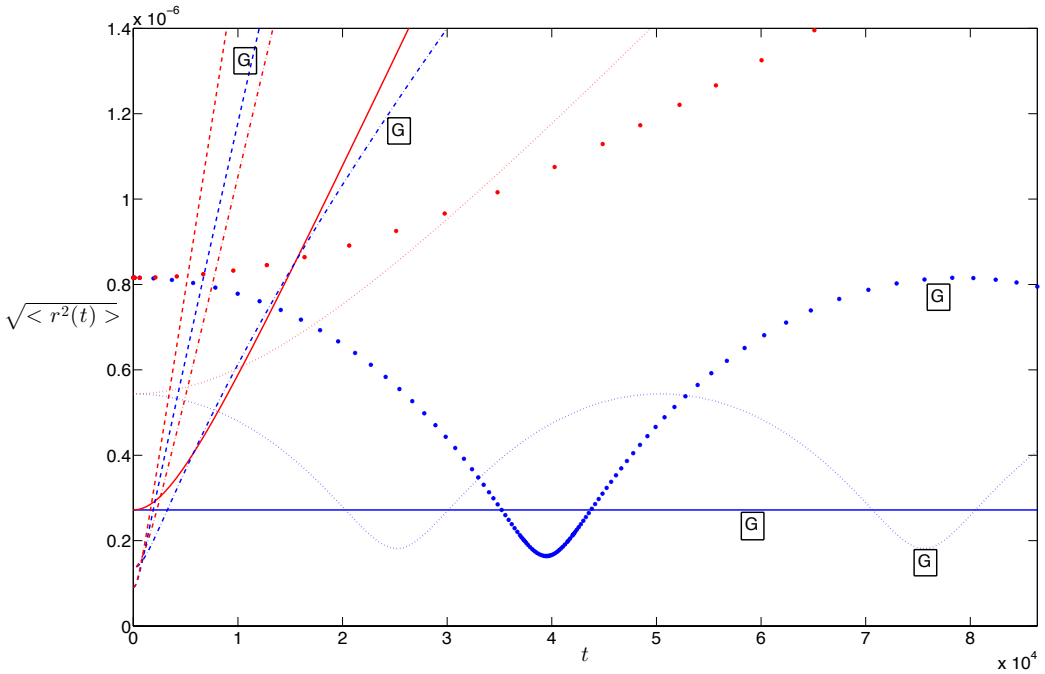

Figure 1: $\sqrt{< r^2 >_t}$ as a function of t for a homogeneous nanosphere of radius 10^{-7} m and mass density 2650 kg m^{-3}, for both the free case and self-gravitating case and for various initial values for the mean width of the state. Identical line styles are shared by the curves with the same initial conditions (moreover the self-gravitational case is labelled by a symbol G inside a square box). The final time corresponds to 24 hours.

arbitrary shape, by the one generated by an "equivalent" step function of same extent. Therefore, in the regime $\sqrt{< r^2 >} \gg 2R$, it is also possible to derive the value of the spring constant by computing the exact self interaction in the region $r < \sqrt{< r^2 >}$, obtained after approximating the CMWF by a step function comprised between the origin and $r = \sqrt{< r^2 >}$ and by imposing analytic continuity on the harmonic potential in the region $r > \sqrt{< r^2 >}$.

Several trajectories generated with the help of our algorithm are plotted in figure 1. The horizontal line in this figure represents a gaussian ground state of the harmonic effective potential mimicking the self-interaction of a gaussian CMWF, as explained above. It can be shown [10] that if the initial spread is smaller than half the spread of the bound state, kinetic energy dominates self-gravitational energy, resulting in a positive total energy, which forces the (spread of the) CMWF to escape to infinity, as seen in figure 1. Breather-type solutions appear when the initial spread of the CMWF is such that the particle is trapped by its own potential.

We also validated our numerical scheme by comparing it to other numerical solutions, such as those obtained by Giulini and Großardt [23] and also those obtained by van Meter [51] for the integro-differential S-N equation (1) in the region $\sqrt{< r^2 >} > 2R$ (the single particle regime). We observed a good qualitative agreement between the predictions made from both approaches, which is perhaps not that amazing as the numerical CMWF solutions of equation (1) considered in [23, 51] have a quasi-gaussian shape.

It is straightforward to analytically[2] estimate the value of the spread of the bound states of the system of equations (5,9,10) (that is, of the static solutions for which free diffusion and the self-gravitational force exactly compensate each other, as given by $dA/dt = 0$) in the extreme regimes $\sqrt{< r^2 >} \ll 2R$

[2]In general however, i.e. outside the extreme regimes $\sqrt{< r^2 >} \ll 2R$ and $\sqrt{< r^2 >} \gg 2R$, the width of the bound state has to be obtained numerically, as explained in [10].

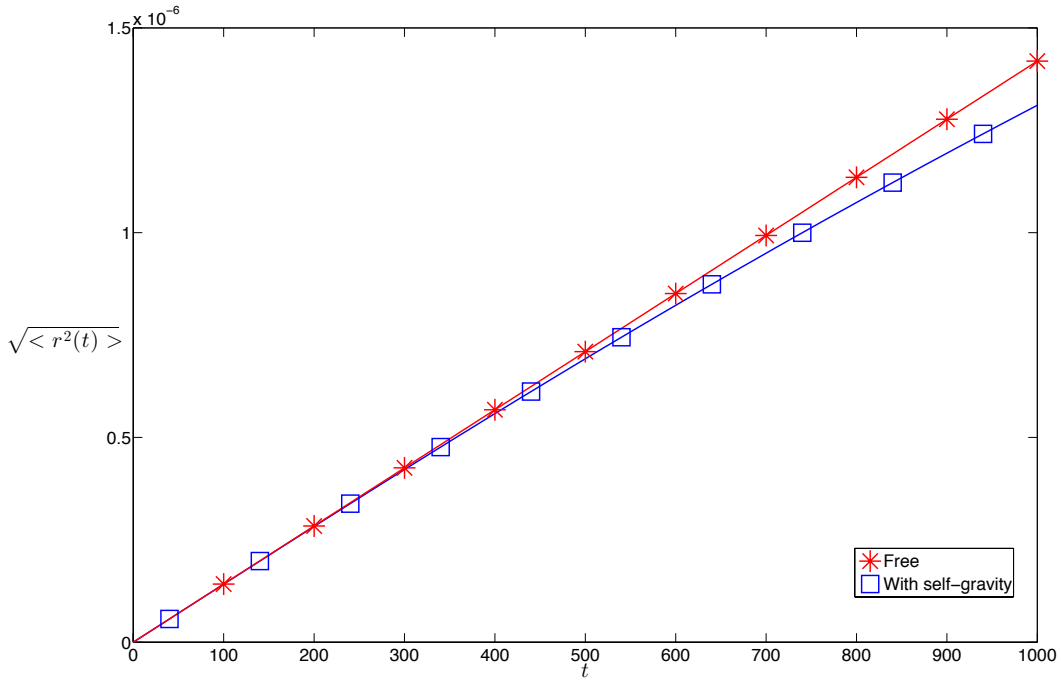

Figure 2: Plot showing the evolution of the average wave packet width for free and self-interacting wave packets as a function of time (in seconds). The mass density of the nanosphere is 2650 kg m^{-3} for a radius of 10^{-6} m. The initial wave packet width is taken to be δx_0=10^{-11} m. A separation of 10^{-7} m between the respective widths occurs after approximately $t = 970$s.

and $\sqrt{< r^2 >} \gg 2R$. In the regime $\sqrt{< r^2 >} \ll 2R$ we find [10]

$$\sqrt{< r_{BS}^2 >} = \frac{9}{4}(\frac{\hbar^2}{GM^3})^{\frac{1}{4}} R^{\frac{3}{4}}, \tag{11}$$

in agreement with Diosi's (rough) predicted value $(\frac{\hbar^2}{GM^3})^{\frac{1}{4}} R^{\frac{3}{4}}$ [11]. There is also good qualitative agreement with the results obtained by more sophisticated methods in the regime $\sqrt{< r^2 >} \gg 2R$, where we find [10]

$$\sqrt{< r_{BS}^2 >} = \frac{9}{4}\frac{\hbar^2}{GM^3}, \tag{12}$$

in agreement with the approximated value of the extent of the ground state given in [23], which is estimated at twice the so-called Lieb radius $\frac{\hbar^2}{GM^3}$ [36]. Furthermore, the numerical value of the energy of the normalized ground state in our approximation is -0.222 $\frac{G^2M^5}{\hbar^2}$, which fits nicely with the value -0.163 $\frac{G^2M^5}{\hbar^2}$ first obtained in [37], which is the best known numerical value for this parameter [7, 28].

In order to estimate the magnitude of the effects due to self-gravity, we first considered an ideal environment in which decoherence is totally absent. We scanned a regime of parameters situated in the mesoscopic transition ($R \approx 100$ nm), and we minimized the free-fall time necessary for discriminating the free and self-interacting regimes, by requiring the free and self-collapsed trajectories to differ by at least[3] 100 nm. In figures 2 and 3 we show the results of our simulations.

[3]Laser interferometry makes it possible for instance to measure positions with a precision of the order of the wavelength of the light emitted by the laser, and 10^{-7} m is a standard wavelength for such applications. In [31] a sub-Rayleigh precision of 40 nm is reported in similar experiments. A precision of 1 nm is reported in [34]. These very precise localisation techniques require one to fit the recorded data with the point-spread-function (PSF) of the optical device used to measure them, which makes it possible to get rid of the Abbe-Rayleigh limit $\delta x \approx \lambda$). Nowadays, they are routinely implemented in biophotonics [34].

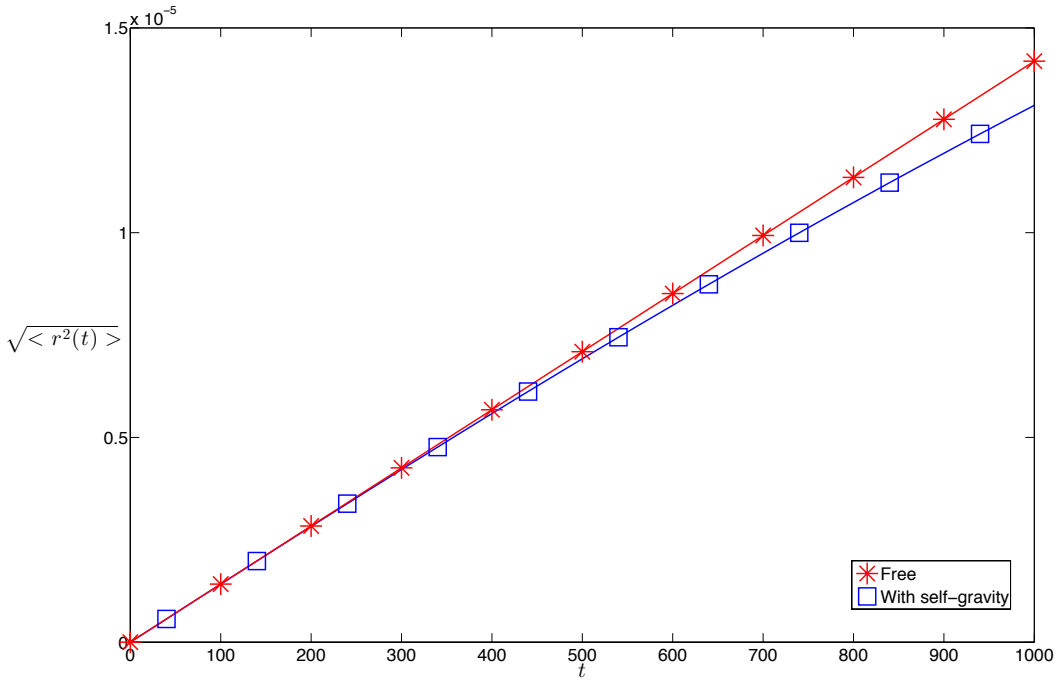

Figure 3: Same as in figure 2, but with a heavier nanosphere. The mass density of the nanosphere is still 2650 kg m^{-3} but its radius is now 10^{-5} m. The initial width of the wave packet is taken to be δx_0=10^{-15} m. A separation of 10^{-7} m between the two widths occurs approximately after $t = 410$s.

To conclude, discriminating free and self-gravitating evolutions, even in the absence of any source of decoherence, would require us to be able to reach free-fall times of the order of say 400 s to 1000 s depending on the radius of the nanosphere (for ten microns and one micron respectively), and to measure the dispersion of positions of freely falling nanospheres with an accuracy of the order of 10^{-7} m. Now, the underlying assumption here is not realistic because a collision with even a single atom (molecule) of the background gas would collapse the CMWF on a distance of the order of the de Broglie wavelength (in our case more or less one Å). Therefore the duration of the free fall must be smaller than the average time between two collisions (γ^{-1} in table 1). In the conditions we work in (see table 1), if we consider the best case of a sphere with a radius of one micron, we find a free fall time of $(4.10^{-1})^{-1} \approx 2.5$ s. This is clearly too small. However, a free fall time of 200 s is allowed for nanospheres with a radius of 100 nm, and in the coming sections we shall examine the possible experimental realisations in this case.

5.2 Interplay between the free Schrödinger evolution and decoherence

In order to take into account the influence of decoherence, we modified (in a first time) the free Schrödinger evolution by assuming that from time to time, the CMWF spatially collapses in accordance with GRW's original model [19]. A key ingredient of this model is the so-called jump factor, that is, a properly normalised Gaussian function $J(x, y, z) = C \exp(-(x^2 + y^2 + z^2)/2\lambda^2))$ (where C is an appropriate normalisation factor) of extent λ centered around (x, y, z). This jump will occur at times that are randomly distributed according to a Poisson distribution with mean τ. The collapse localisation (x_0, y_0, z_0) is also randomly distributed with a spatial probability distribution given by

$$\rho(x_0, y_0, z_0) = \int_{R^3} dxdydz |J(x_0 - x, y_0 - y, z_0 - z)\Psi(x, y, z)|^2. \tag{13}$$

During a jump, the initial CMWF ψ_i changes to $\psi_f(x,y,z) = J(x,y,z)\psi_i(x,y,z)/\sqrt{\rho(x,y,z)}$. In particular, gaussian states of the form

$$\Psi_i(t,\mathbf{x}) = \exp(-Ar^2 + B_x x + B_y y + B_z z + C) \tag{14}$$

jump to shrunken gaussian states of the form

$$\Psi_f(t,\mathbf{x}) = \exp(-(A+(\alpha/2))r^2 + B'_x x + B'_y y + B'_z z + C') \ . \tag{15}$$

This model is characterized by two constants: $\gamma = 1/\tau$ (the inverse of the average time between two jumps or localisations) and the inverse of a squared length $\alpha = 1/\lambda^2$ where λ is the extent of the localisation region. Many important properties of the model only depend on the product of γ and α, which is denoted by Λ :

$$\Lambda = \gamma \cdot \alpha \, . \tag{16}$$

In particular [19], in the limit where we let γ become arbitrarily large, keeping Λ fixed, the CMDM ρ obtained after averaging over various realizations of the localisation process obeys a Lindblad type equation of the type

$$\frac{d\rho(t)}{dt} = -\frac{i}{\hbar}[\hat{H},\rho(t)] - \frac{\Lambda}{4}\sum_{i=1,2,3}[\hat{q}_i,[\hat{q}_i,\rho(t)]], \tag{17}$$

where $\hat{H}$ denotes the free Hamiltonian and where q_1, q_2, q_3 represent the three components of the position operator in Cartesian coordinates. This equation appears in numerous models of decoherence, exotic ([5],[19],[22]) as well as non-exotic [30, 47], and is typical of the long wavelength (LWL) regime $\lambda \gg \sqrt{< r^2 >}$ in which the region of localisation is quite larger than the size of the object (i.e., than the extent of individual CMWFs). Several jumps are then necessary in order to affect the extent of the wave function. In the short wavelength regime however, i.e., in the limit where $\lambda \ll \sqrt{< r^2 >}$, the CMDM obeys the von Neumann equation [19]

$$\frac{d < \hat{q}'_i|\rho(t)|\hat{q}''_j >}{dt} = \frac{i\hbar}{2m}(\frac{\partial^2}{\partial^2 q'_i} - \frac{\partial^2}{\partial^2 q''_j})\rho(t) - \lambda < \hat{q}'_i|\rho(t)|\hat{q}''_j > . \tag{18}$$

The advantage of the GRW Monte Carlo-type unravelling of the decoherence process is that it contains both regimes (both master equations above) as limiting cases, which makes it also an excellent model for mimicking non-exotic decoherence [50] in the case where, throughout the evolution, the system would pass through different regimes (SWL and LWL). For instance, let us assume that the spread of the CMWF is comprised in the nano to micrometer range. If we consider scattering by the nanosphere of residual gas molecules, λ will be equal to the de Broglie wavelength of air molecules, i.e. of the order of 0.15 nm at a temperature of 4.5 K, which corresponds to the SWL regime. In practice, the GRW localisation length (10^{-7} meter) will be longer than the size of the CMWF and we will be in the LWL regime if we operate at nanoscales, while at microscales we find ourselves in the SWL regime.

In absence of self-gravitation the effects of decoherence are well-known: at each jump the center of the wave packet jumps at random while its extent simultaneously shrinks. Indeed, the values of A before (A_i) and after the jump (A_f) are related by the relation $A_f = A_i + \alpha/2$. As the extent δr of the CMWF is of the order of $1/\sqrt{Re(A)}$, we find, neglecting dimensional factors of the order of unity, that the extents of the CMWF after and before a jump are related through the rule $1/\delta r_f^2 = 1/\delta r_i^2 + \alpha$ such that $\delta r_f - \delta r_i \approx -\alpha \delta r_i^3$. Between two jumps the wave packet diffuses according to the free Schrödinger evolution and $\delta r(t+\tau) \approx \delta r(t) + \hbar\tau/(M\delta r)$, where $\tau = \gamma^{-1}$ is the average time between two jumps. After a while the spread of the wave packet asymptotically reaches an equilibrium value for which the shrinking is compensated by free diffusion: $-\alpha\delta r^3_{equil.} \approx -\hbar\tau/(M\delta r_{equil.})$. The asymptotic value of the spread of the CMWF reads thus [19, 5]

$$\delta r_{equil.} = (\hbar/M\alpha\gamma)^{1/4} = (\hbar/M\Lambda)^{1/4}. \tag{19}$$

Of course, experimentally, we have no access to the individual trajectories followed by the CMWF, but averaging over numerous realizations of the stochastic localization mechanism by a quantum Monte-Carlo procedure makes it possible to predict the average evolution of the object, that is of the associated CMDM. As shown in the original GRW paper, globally, the spread of the CMDM diffuses

even faster than in absence of jumps, because of the dispersion of the positions at which jumps occur, according to the formula [19, 47]:

$$\sqrt{< r^2 > (t)} = \sqrt{< r^2 > (0)} \cdot \sqrt{1 + \frac{9\hbar^2 t^2}{4M^2(< r^2 > (0))^2} + \frac{\Lambda \hbar^2 t^3}{2M^2 < r^2 > (0)}}. \quad (20)$$

This relation is important because it makes it possible to estimate the value of the decoherence parameter Λ (obtained after summing the exotic and possibly non-exotic contributions: $\Lambda = \Lambda_{exotic} + \Lambda_{non-exotic}$). It explains in particular why we can obtain direct information about the decoherence undergone by the microsphere, simply by measuring the spread of its CMDM.

We evaluated the parameters γ and α (and Λ) corresponding to various exotic and non-exotic decoherence processes. In a first time, we considered three non-exotic processes: scattering of ambient air molecules by the nanosphere and scattering of environmental thermal photons, as well as emission of thermal photons by the nanosphere at temperature T_i [47, 42].

5.2.1 Decoherence due to residual gas

Decoherence due to scattering by the nanosphere of ambient gas molecules is characterized by the parameters $\alpha_{air} = 1/\lambda_{air}^2 = m_a k_B T/2\pi\hbar^2 \approx 10^{19} T$ (where m_a is the average atomic mass of an air molecule, k_B the Boltzmann constant and T the ambient temperature [42] expressed in kelvin) and $\Lambda_{air} = \frac{8\sqrt{2\pi}}{3\sqrt{3}} \frac{m_a \overline{v}_a p R^2}{\hbar^2}$ where $\overline{v}_a$ is the average velocity of the gas molecules and p their pressure [47]. At normal pressure, $\gamma_{air} \approx 10^{28} \mathrm{s}^{-1} R^2 T^{1/2}$, where R is the radius of the sphere expressed in meters and T the temperature. At very low pressure (10^{17} times less than the atmospheric pressure, which corresponds to a density of some hundreds of molecules by cm^3) we find $\gamma_{air} \approx 10^{11} \mathrm{s}^{-1} R^2 T^{1/2}$ and $\Lambda_{air} \approx 10^{30} R^2 T^{3/2}$.

5.2.2 Decoherence due to thermal photons

Decoherence due to black body (b.b.) photons that stem from the environment is characterized by the parameters $\alpha_{bb}^{scattering} = (k_B T/(\pi^{3/2}\hbar c))^2 \approx 4 \times 10^4 T^2$, $\Lambda_{bb}^{scattering} \approx 10^{36} \mathrm{m}^{-2}\mathrm{s}^{-1} R^6 T^9$ [47]. Decoherence due to black body photons emitted by the nanosphere heated in the trap at a temperature T_i has also been considered (see e.g. ref.[42]), leading to the parameters $\alpha_{bb}^{emission} \approx 4 \times 10^4 T_i^2$, and $\Lambda_{bb}^{emission} \approx (5/6) \times 10^9 R^3 T^6 \mathrm{m}^2\mathrm{s}^{-1}$. In [43], an internal nanosphere temperature $T_i = 206K$ was considered, leading to $\alpha_{bb}^{emission} \approx 1.6 \times 10^9$ and $\Lambda_{bb}^{emission} \approx 5 \times 10^{22} R^3 \mathrm{m}^2\mathrm{s}^{-1}$.

In [32] it is mentioned that a temperature $T_i < 20$ K is realizable thanks to a thermal shield installed inside the satellite, in which case $\alpha_{bb}^{emission} \approx 1.6 \times 10^7$ and $\Lambda_{bb}^{emission} \approx 5 \times 10^{16} R^3 \mathrm{m}^2\mathrm{s}^{-1}$. Together, the above results make it possible to estimate the various non-exotic decoherence parameters due to environmental influence. Some decoherence parameters representative of these various mechanisms of decoherence are listed in table 1 in function of various values for the radius of the nanosphere.

R	gas scattering		b. b. scattering		b. b. emission		$\Lambda_{crit.}$
	Λ_{gas}	γ_{gas}	$\Lambda_{b.b.}^{scatt.}$	$\gamma_{b.b.}^{scatt.}$	$\Lambda_{b.b.}^{emission}$	$\gamma_{b.b.}^{emission}$	
10^{-5}	6.4×10^{21}	4×10^{1}	6.5×10^{16}	6.5×10^{9}	5×10^{1}	3×10^{-6}	10^{17}
10^{-6}	6.4×10^{19}	4×10^{-1}	6.5×10^{10}	6.5×10^{3}	5×10^{-2}	3×10^{-9}	10^{14}
10^{-7}	6.4×10^{17}	4×10^{-3}	6.5×10^{4}	6.5×10^{-3}	5×10^{-5}	3×10^{-12}	10^{11}
10^{-8}	6.4×10^{15}	4×10^{-5}	6.5×10^{-2}	6.5×10^{-9}	5×10^{-8}	3×10^{-15}	10^{-22}

Table 1: Table of non-exotic decoherence parameters estimated for a nanosphere of unspecified density. On the right, we also mention the value of $\Lambda_{crit.}$ (for the case of 2.6 times normal density) which is an effective decoherence measuring the strength of self-gravity (cf. the discussion of equation (24)) . The non-exotic parameters were evaluated at a temperature T_i of 20 K, in an environment at temperature 16 K. Λ is expressed in $\mathrm{m}^{-2}\mathrm{s}^{-1}$, the radius R in m and γ in s^{-1}.

Throughout the paper we shall often assume that the density of the nanosphere is equal to the density of silicate, as described in [44], which is equal to 2.6 times the normal (water) density. At the mesoscopic transition $R \approx 10^{-7}$m, the mass of the nanosphere is then of the order of 10^{-17}kg and counts approximately 10^{10} nucleons. Sometimes we shall aslo consider a density more or less ten times higher, because this increases self-gravitation such that the mesoscopic transition will occur at a slightly smaller radius, as has been shown in [10]. Such a density corresponds to the density of gold which is also a realistic candidate for our experimental proposal due to the fact that gold nanoparticles of various shapes (among others gold nanospheres) are nowadays used on a massive scale in medical and biological applications.

Even though the decoherence parameter Λ due to residual gas dominates the others, all these mechanisms of decoherence must be taken into account and the various parameters do play a role. For instance, if γ is smaller than the inverse of the free-fall time, no jump is likely to occur and it is consistent to neglect the corresponding source of non-exotic decoherence. This is the case for the non-exotic contributions in the experimental set up described here, whenever we consider free-fall times of the order of 100 s and nanospheres of radius of the order of 100 nm, as is clear form table 1. The probability that a collision with a residual gas molecule or the emission or scattering of a b.b. photon occurs during the free-fall is then very close to 0 and can consistently be neglected. However, in that case other decoherence mechanisms, for instance those due to exotic sources of decoherence, must be considered in priority, which opens an interesting observational window around the mesoscopic transition where non-standard effects are likely to prevail.

5.2.3 Exotic decoherence from four SL models

We also considered four SL models. In the original GRW model [19] – according to which γ_{GRW} is equal to the number of nucleons of the nanosphere times the universal parameter γ_0 chosen by GRW to be equal to 10^{-16} s^{-1} – one has that $\Lambda_{GRW} = \alpha_{GRW}\gamma_{GRW}$=$10^{-14}m^{-2}\gamma_{GRW}$. In turn, in the CSL model [22], γ_{CSL} is equal to the square of the number of nucleons of the nanosphere, multiplied by times the same universal parameter γ_0 and by a scale dependent function of the form $\tilde{f}_{CSL} = (3/2)(10^{-7}/R)^4[1 - 2(10^{-7}/R)^2 + (1 + 2(10^{-7}/R)^2)e^{-R/10^{-7}}]$.

Although the Lindblad equation (17) can be derived from a process *à la* GRW where sudden jumps happen from time to time, it can also be derived from a quantum Monte Carlo unravelling in the sense of Ito, which is *per se* a continuous stochastic process. This is the case of the CSL model where by construction no sudden quantum jump is likely to occur, which justifies the "C" label of the CSL model. When the GRW model operates in the LWL regime, and provided the jump rate is high enough[4], the GRW and CSL models are equivalent in the sense that in both approaches the averaged CMDM obeys equation (17).

The decoherence parameters of the QG model [15, 16] obey $\Lambda_{QG} = \frac{c^4 M^2 m_0^4}{\hbar^3 m_P^3}$ where m_P is the Planck mass, M is the mass of the nanosphere, m_0 the mass of a nucleon and for which $\alpha_{QG} = \frac{c^2 m_0^4}{\hbar^2 m_P^2} \approx 10^{-6}$m^{-2}, $\gamma_{QG} \approx 3 \times 10^5 (M/m_0)^2$s^{-1} and typically $\Lambda_{QG} \approx 3 \times 10^{19}(M/10^{-17}\text{kg})^2$.

The decoherence parameters of the Diosi Penrose (DP) model obey $\Lambda_{DP} = GM^2/(2R^3\hbar)$ and $\alpha = R^{-2}$ (where R is the radius of the sphere and M its mass [13, 41, 42]) as well as $\gamma_{DP} = GM^2/(2R\hbar)$.

Some decoherence parameters predicted in the framework of these models are given in table 2, in function of various values for the radius of the nanosphere.

[4]It is worth noting that, as is clear from table 2, the typical time between two jumps predicted by the original GRW model is much longer than the duration of the experiment we propose. It is therefore obvious that our proposal will not discriminate the GRW model, or at least its original parameters. Actually, to date, no experimental discrimination of these parameter values has been realized [17]. Our approach however complements several indirect observations which seriously constrain the allowed range of parameters in the original GRW model. These include for instance diffraction (interference) experiments, measures of universal warming, spontaneous X-ray and sound emission, decay of supercurrents and so on (see [17] for a review).

R	GRW		CSL		QG		DP		$\Lambda_{crit.}$
	Λ_{GRW}	γ_{GRW}	Λ_{CSL}	γ_{CSL}	Λ_{QG}	γ_{QG}	Λ_{DP}	γ_{DP}	
10^{-5}	6×10^{13}	6×10^{-1}	5×10^{21}	5×10^{7}	3×10^{31}	3×10^{37}	5×10^{19}	5×10^{9}	10^{17}
10^{-6}	6×10^{10}	6×10^{-4}	5×10^{19}	5×10^{5}	3×10^{25}	3×10^{31}	5×10^{16}	5×10^{4}	10^{14}
10^{-7}	6×10^{7}	6×10^{-7}	2.5×10^{18}	2.5×10^{4}	3×10^{19}	3×10^{25}	5×10^{13}	5×10^{-1}	10^{11}
10^{-8}	6×10^{4}	6×10^{-10}	10^{16}	10^{2}	3×10^{13}	3×10^{19}	5×10^{10}	5×10^{-6}	10^{-22}

Table 2: Parameter values in four exotic decoherence models, estimated for a nanosphere of 2.6 times the normal density. We also mention the value of $\Lambda_{crit.}$ evaluated at this same density. Λ is expressed in $\mathrm{m}^{-2}\mathrm{s}^{-1}$, the radius R in m and γ in s^{-1}.

5.2.4 Tests of macrorealism

Whenever exotic decoherence is at least of comparable magnitude as environmental decoherence, a crucial test of macrorealist models becomes possible, in principle, provided these models lead to a measurable difference in the spread of the wave function (which, in the following, we conservatively[5] take to be at least 5 nm). In figures 4 and 5, we plotted the spread of the wave function for the center of mass for nanospheres with a 100 nm radius, after a free fall of 1000s, for two different initial spreads, in the presence (upper curve) and absence (lower curve) of strong exotic decoherence. Obviously, the influence of exotic decoherence is measurable when γ is strong enough (of the order of 10^{18} and more), which establishes that our experimental proposal can unambiguously reveal the hypothetical presence of exotic decoherence in the case of the CSL or QG models (compared to the DP and GRW parameter values plotted in table 2, these can be qualified as "strong" SSL models).

As has been noted in [42], SL models invoking self-gravitation and/or fluctuations of the space time metric are a lot weaker than the CSL and QG gravity models. If the experiment we propose is realized in an environment prepared at a temperature of 16 K, in extreme vacuum conditions, exotic decoherence as predicted in the DP model [42, 12, 13, 41] would be stronger than the non-exotic decoherence due to the environment[6] whenever the radius of the nanosphere is of the order of 100 nm. Therefore its presence is in principle measurable. We shall come back to this point in section 6 which is devoted to the numerical results. Before doing so however, we shall consider the joint influence of decoherence and self-gravitation.

5.3 Interplay between Self-Gravitation and Decoherence

We learn from table 1 that when the radius of the nanosphere becomes larger than one micron, collisional decoherence is unavoidably present. Unfortunately, this means that the results presented in figures 2 and 3 (corresponding to radii of one and ten microns respectively) and where self-gravitation is assumed to be acting in a totally clean (decoherence-free) environment, do not correspond to a realistic situation. For smaller radii, self-gravitation is weaker and most often would only lead to measurable effects after free falls longer than several thousands of seconds[7], as can be seen from figure 1. Actually, even in the absence of decoherence, the incidence of self-gravitation at the level of the spread of the CMWF, which is the experimental parameter that we privilege in our approach, remains weak and difficult to observe. This is because in order to enhance self gravitation we must increase the mass of the wave packet, which slows down the free diffusion and ultimately imposes times of free flight that are too long to be realized experimentally. If in turn, we try to accelerate the spread of the CMWF by decreasing the initial spread, we increase the kinetic energy of the particle and self-gravitation weakens relatively to free diffusion.

[5] Nanometer accuracy has been reported in Ref.[34].

[6] As can be seen from the comparison of tables 1 and 2, environmental photons cause a much weaker decoherence. The decoherence parameter Λ due to gas molecules is quite large but the average time between two jumps is in this case of the order of 250 s. Therefore, provided we realize the experiment in 200 s, the influence of the background gas can be kept under control.

[7] Figures 2 and 3 were obtained after minimizing the flight time (over the set of experimentally reachable adjustable parameters such as the size of the nanosphere and the initial spread of the CMWF) needed to observe a discrepancy of 100 nm after 1000 s between free and self-gravitating trajectories.

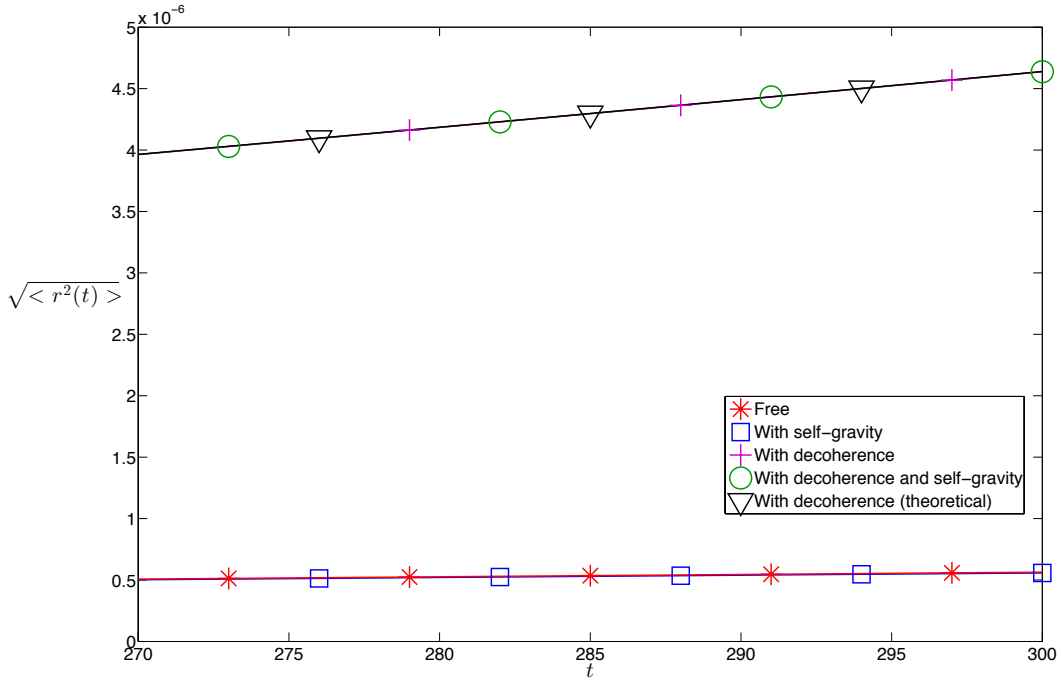

Figure 4: Spread (in m) of the CMDM for $t \in [270, 300]$, for a nanosphere of radius 100 nm and mass density $\rho = 20000\,\mathrm{kg\,m^{-3}}$ (density of gold), with initial spread $\delta r_0 = 10^{-9}$ m. The curves marked by squares and stars correspond to the absence of decoherence, respectively with and without self-gravity. The decoherence parameters are $\alpha = 10^{18}$ m^{-2} and $\gamma = 1$ s^{-1}. The curves marked by plus symbols and circles respectively correspond to the absence and presence of self-gravity, while the curve marked by triangles is the analytic curve (20).

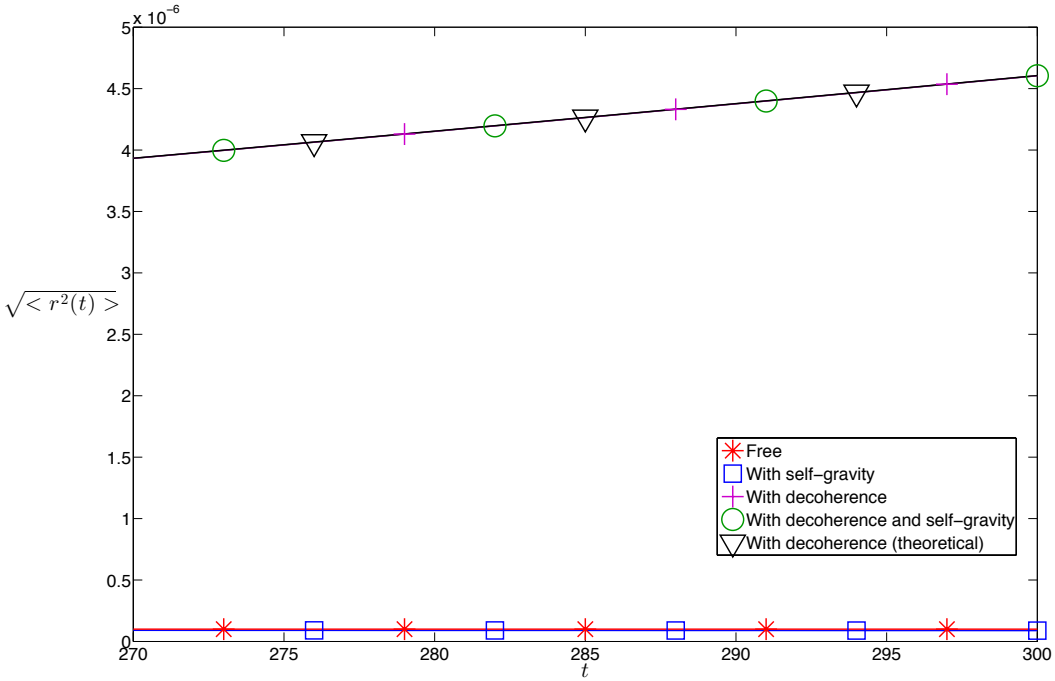

Figure 5: Spread (in m) of the CMDM for $t \in [270, 300]$, for a nanosphere of radius 100 nm and mass density $\rho = 20000\,\mathrm{kg\,m^{-3}}$ (density of gold), with initial spread $\delta r_0 = 10^{-7}$ m. The curves marked by squares and stars correspond to the absence of decoherence, respectively with and without self-gravity. The decoherence parameters are $\alpha = 10^{18}$ m^{-2} and $\gamma = 1$ s^{-1}. The curves marked by plus symbols and circles respectively correspond to the absence and presence of self-gravity, while the curve marked by triangles is the analytic curve (20).

The situation however could improve in the presence of decoherence, which modifies the diffusion process, in such a way that one can experimentally consider heavier (larger) nanospheres for which self gravitation becomes stronger as well. More precisely, we expect that decoherence maximally amplifies the influence of self-gravity in the case where the localisation mechanism repeatedly shrinks the CMWF to a size where self gravitation actively slows down the free expansion of the CMWF, as is confirmed in our numerical study. In this case, the evolution between two successive jumps is expected to get maximally disturbed by self-gravitation. This occurs whenever $\delta r_{equil.}$, the asymptotic[8] spread (19) associated to decoherence is comparable in size to $\sqrt{< r_{BS}^2 >}$, the static, self-collapsed radius (given by (11) or (12), depending on the situation)

$$\delta r_{equil.} = \sqrt{< r_{BS}^2 >}. \tag{21}$$

From this constraint, combining equations (11), (12) and (19)), it is straightforward to derive an analytic estimate of the critical decoherence parameter for which self gravitation and decoherence have comparable magnitudes. This critical decoherence parameter $\Lambda_{crit.}$ reads (neglecting constant dimensional factors of the order of unity)

$$\Lambda_{crit.} = \frac{G^4 M^{11}}{\hbar^7} \tag{22}$$

in the single particle regime $\sqrt{< r_{BS}^2 >} \gg 2R$, and

$$\Lambda_{crit.} = \frac{G M^2 R^{-3}}{\hbar} \tag{23}$$

in the macroscopic regime $\sqrt{< r_{BS}^2 >} \ll 2R$.

In summary, decoherence will not mask self-gravitation whenever $\Lambda_{crit.}$ is larger than Λ, i.e. whenever

$$\Lambda_{crit.} \geq \Lambda, \tag{24}$$

Different values of $\Lambda_{crit.}$ are plotted in tables 1 and 2, and it is instructive to compare them with the other decoherence parameters.

It is also instructive to reconsider the problem in the framework of the aforementioned QMUPL model [5, 13], where the stochastic parameters only affect the center of a gaussian wave packet, not its size, and for which it can be shown that for a gaussian ansatz of the form $\Psi(t, \mathbf{x})$=exp$(-Ar^2 + B_x x + B_y y + B_z z + C)$, $A(t)$ evolves deterministically according to

$$\frac{dA(t)}{dt} = \frac{-2i\hbar A^2}{M} + \Lambda. \tag{25}$$

On the other hand, as we have explained, A evolves deterministically according to (6) when only self gravitation is present. Taking into account both contributions, we find that in the simultaneous presence of decoherence and self-gravity, $A(t)$ obeys the evolution law

$$\frac{dA(t)}{dt} = \frac{-2i\hbar A^2}{M} + \frac{ik(< r^2 >)}{2\hbar} + \Lambda. \tag{26}$$

It is easily verified that $\Lambda_{crit.}$ satisfies $\frac{k(<r_{BS}^2>)}{2\hbar} = \Lambda_{crit.}$, which sheds a new light on the conditions (21–23). It is worth stressing that, in agreement with the remark made in footnote 8, the regime considered here is a LWL regime for which the jump rate is very high. Indeed, the QMUPL model can be derived from the GRW model in the limiting case where we let γ become arbitrarily large, keeping the product $\gamma.\alpha$ fixed: $\gamma \to \infty$, $\gamma.\alpha$=const.=Λ.

[8] It is crucial to note that this asymptotic value corresponds to an equilibrium situation which establishes itself only after sufficiently many jumps have occured. Therefore, the present analysis is only valid whenever the duration of the experiment is significantly longer than the average time lapse between two jumps.

6 Numerical predictions.

Summarizing the discussions of the previous sections: as is clear from tables 1 and 2, there exists only a tiny window around the mesoscopic transition ($R = 10^{-7}$m) where self-gravity and/or macrorealism are likely to be falsifiable. For nanospheres of smaller radii, self-gravity and exotic decoherence become too weak very rapidly, while for larger radii they become overwhelmed by environmental decoherence. It is also obvious that strong exotic (CSL and QG) decoherence, if these exist, will always mask the presence of self-gravity and that it is only in the absence of such strong sources of exotic decoherence that self gravity will be falsifiable. Experiments will therefore have to be conducted in two steps. In a first time, one must check whether or not "strong" exotic decoherence (of the CSL or QG types and, as we shall soon show, of the DP type as well) is present. If the answer is negative, it becomes possible to falsify self gravitation. Needless to say, a positive answer in the first or second case would constitute a remarkable achievement in itself.

In figures 4 through to 14, we plot the temporal evolution of the spread of CMDMs in the presence of decoherence. The results presented in these plots were obtained by mixing a large number[9] of individual trajectories in which the CMWF jumps, from time to time, *à la* GRW and where in-between two jumps, it evolves according to either the free Schrödinger equation or to the approximated S-N equation (5). Due to computational time limitations, in order to make our calculations tractable we kept the parameter γ relatively low (one jump every second, except in the case presented in the last figure[10]) and we adapted in each case the value of $(\alpha = \Lambda/\gamma)$ in order to reach the values of Λ found in tables 1 and 2. We checked however, after averaging over many realizations of the GRW process, that the results we obtain in absence of self-gravity remain close to the theoretically predicted asymptotic value (20), thus confirming that the GRW model, as is well known, is to some extent independent of variations in γ and α provided $\Lambda = \alpha\gamma$ remains constant. (In all the figures $4 \sim 14$, we also plot each time the theoretical estimate (20) of the asymptotic spread in the limit where the spread of the CMDM is averaged over infinitely many realisations of the stochastic jump process.)

Our simulations confirm the various effects we predicted in the previous sections on the basis of purely theoretical considerations:

(i) exotic decoherence is certainly likely to be revealed by the free fall experiment we propose in the "strong" exotic decoherence regimes, as predicted by the CSL and QG models. In such regimes, self gravity is clearly overwhelmed by decoherence. This can be seen from pictures 4 and 5 where the curves in the absence (below) and presence (above) of decoherence are very clearly distinguishable. The curves with/without decoherence in these figures differ by more or less 500 nm after 300 s, which shows that even after a mere 100 s, the experiment would make it possible to falsify without any doubt the CSL and QG models.

(ii) it is in fact also possible to falsify the "weak" DP model in the same way as the strong models. This can be seen from figure 6 (for a silicate nanosphere) where the curves in the absence or presence of decoherence are still distinguishable: they are separated by a distance of the order of 50 nm after 200 s, which is still largely within the range of sensitivity of 5nm we consider. Obviously decoherence masks self-gravity here as well, which is not suprising since the DP decoherence parameter exceeds the critical parameter by a factor 100.

(iii) From figures $7 \sim 11$ (in the presence of self-gravity, for a gold nanosphere) it is clear that the subtle interplay between self-gravity and decoherence we predicted theoretically in the previous section is manifestly present: the effect of self-gravitation in the presence of decoherence remains comparable to the effect it has in the case without decoherence, whenever the decoherence remains close to the critical decoherence parameter (figures 7, 8 and 9). When decoherence increases further (figures 10 and 11) it is obvious that decoherence will mask self-gravity. In other words, for a certain range of decoherence, self-gravitational effects are robust with respect to decoherence.

(iv) it is not possible to falsify the "weak" DP model in the absence of self-gravity when the initial spread of the CMDM is too small (see also point vi) below). This can be seen, for example, from

[9] This is necessary because the spread is itself a stochastic variable distributed in accordance with the law of large numbers.

[10] Obviously this rate is considerably higher than the rate derived from the GRW model but which is anyhow so low in the regimes of size and mass that we investigate that, as already noted (footnote 4), the GRW model is out of reach in our proposed experiment.

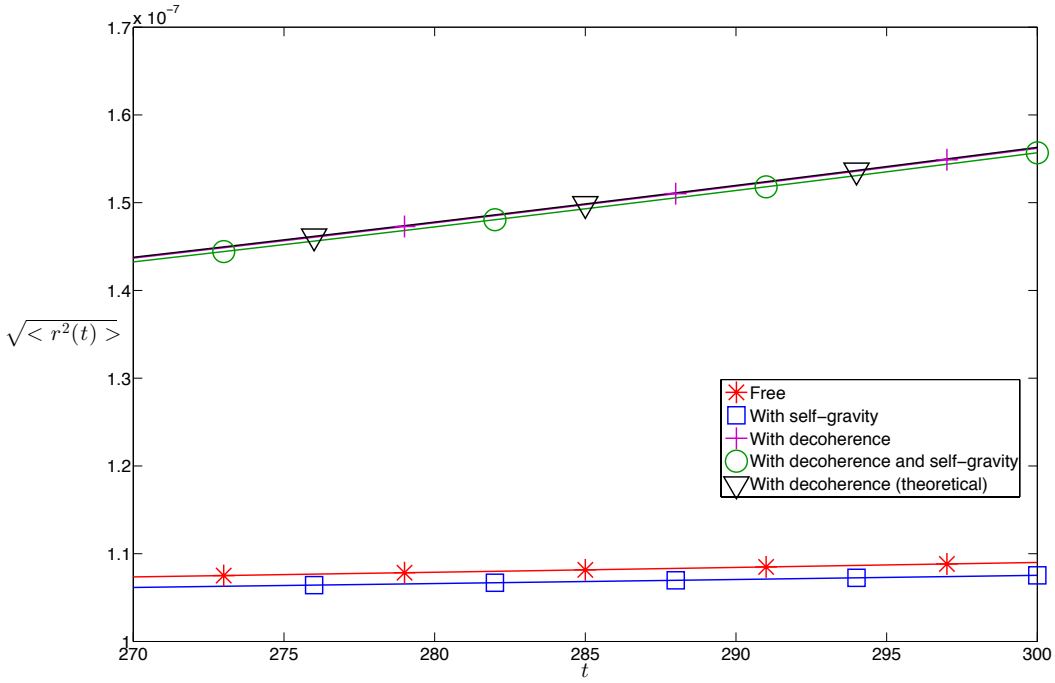

Figure 6: Spread (in m) of the CMDM for $t \in [270, 300]$, for a nanosphere of radius 100 nm and mass density $\rho = 2600\,\mathrm{kg\,m^{-3}}$ (density of silicate), with initial spread δr_0=10^{-7} m. The curves marked by squares and stars correspond to the absence of decoherence, respectively with and without self-gravity. The decoherence parameters are $\alpha = 10^{13}$ m^{-2} and $\gamma = 1$ s^{-1}. The curves marked by plus symbols and circles respectively correspond to the absence and presence of self-gravity, while the curve marked by triangles is the analytic curve (20).

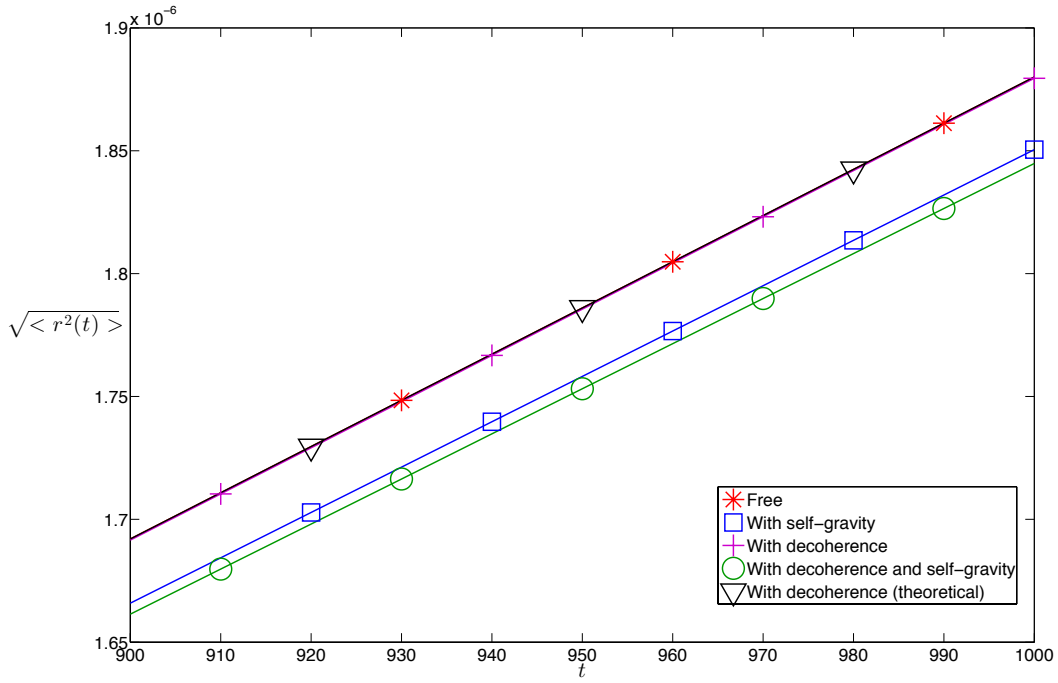

Figure 7: Spread (in m) of the CMDM for $t \in [900, 1000]$, for a nanosphere of radius 100 nm and mass density $\rho = 20000\,\mathrm{kg\,m^{-3}}$ (density of gold), with initial spread δr_0=10^{-9} m. The curves marked by squares and stars correspond to the absence of decoherence, respectively with and without self-gravity. The decoherence parameters are $\alpha = 10^{11}$ m^{-2} and $\gamma = 1$ s^{-1}. The curves marked by plus symbols and circles respectively correspond to the absence and presence of self-gravity, while the curve marked by triangles is the analytic curve (20).

figure 9 (or 7 or 8) where in the absence of self-gravitation, although still distinguishable, the curves corresponding to the cases in which decoherence is either absent or present are only separated by a distance of the order of a nanometer after 1000 s. This sort of precision is of course is out of reach in our proposal.

It is however possible to falsify the "weak" DP model in the presence of self-gravity. Indeed, the distance between the corresponding curves (labeled "free" and "with decoherence and self-gravity") in figure 9 is of the order of 20 nm after 1000 s, which is right at the edge of presently reachable precision as we must limit ourselves to free fall times of the order of 200 s (to avoid decoherence caused by background gas). The effect would be easier to detect however if the pressure could be decreased, e.g. increasing the maximal free fall time by a factor of, say, 5. Then, as the difference between the predicted spread in the presence of self-gravity and decoherence and the predicted spread in the presence of self-gravity only is of the order of 10 nm after 1000 s, it would in principle even be possible to distinguish both behaviours. Remarkably, self-gravity even amplifies the effect of decoherence here because the difference between the predicted spread in the presence of self-gravity and decoherence and the predicted spread in the presence of self-gravity only, is more or less ten times higher than what we would get in the absence of self-gravity where only a difference of the order of one nanometer is predicted.

(v) Besides the limited precision of individual position measurements, another problem arises if the difference in spread that is to be measured is too small: due to the law of large numbers (as mentioned in footnote 9) the acquisition time necessary for an evaluation of the spread with a precision of ϵ, increases as $1/\epsilon^2$. For instance, discriminating a 100 nanometer and a 99 nanometer spread would impose a measurement with a precision of 0.1 nanometer. This would require us, by virtue of the law of large numbers, to repeat free falls one million times ($=(0.1/100)^{-2}$), which is clearly not possible.

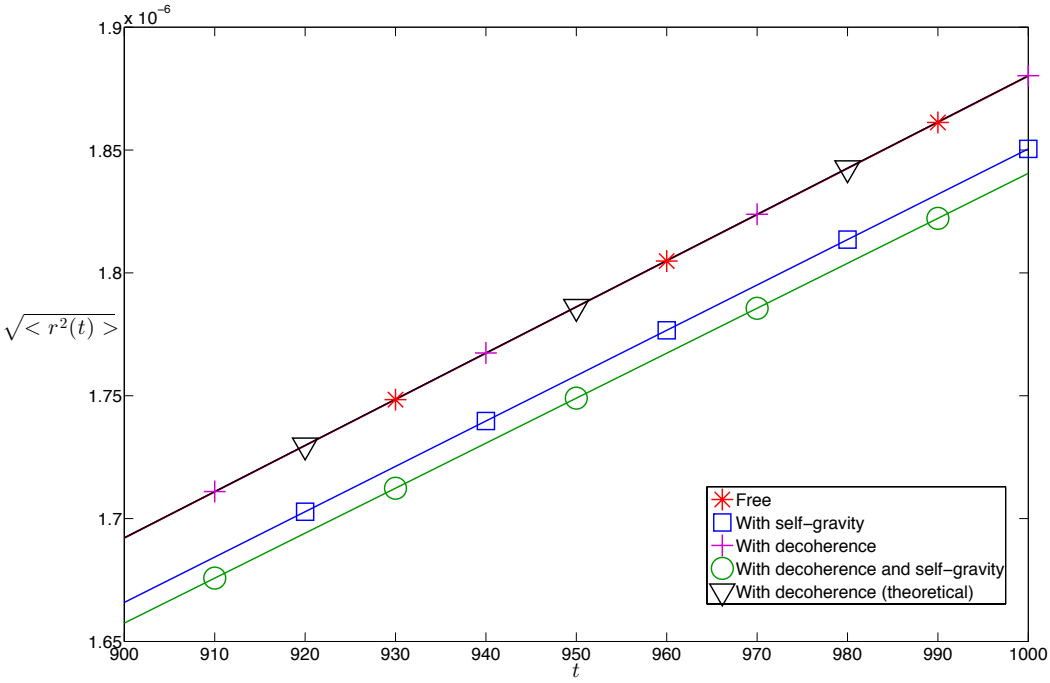

Figure 8: Spread (in m) of the CMDM for $t \in [900, 1000]$, for a nanosphere of radius 100 nm and mass density $\rho = 20000\,\mathrm{kg\,m^{-3}}$ (density of gold), with initial spread δr_0=10^{-9} m. The curves marked by squares and stars correspond to the absence of decoherence, respectively with and without self-gravity. The decoherence parameters are $\alpha = 10^{12}$ m^{-2} and $\gamma = 1$ s $^{-1}$. The curves marked by plus symbols and circles respectively correspond to the absence and presence of self-gravity, while the curve marked by triangles is the analytic curve (20).

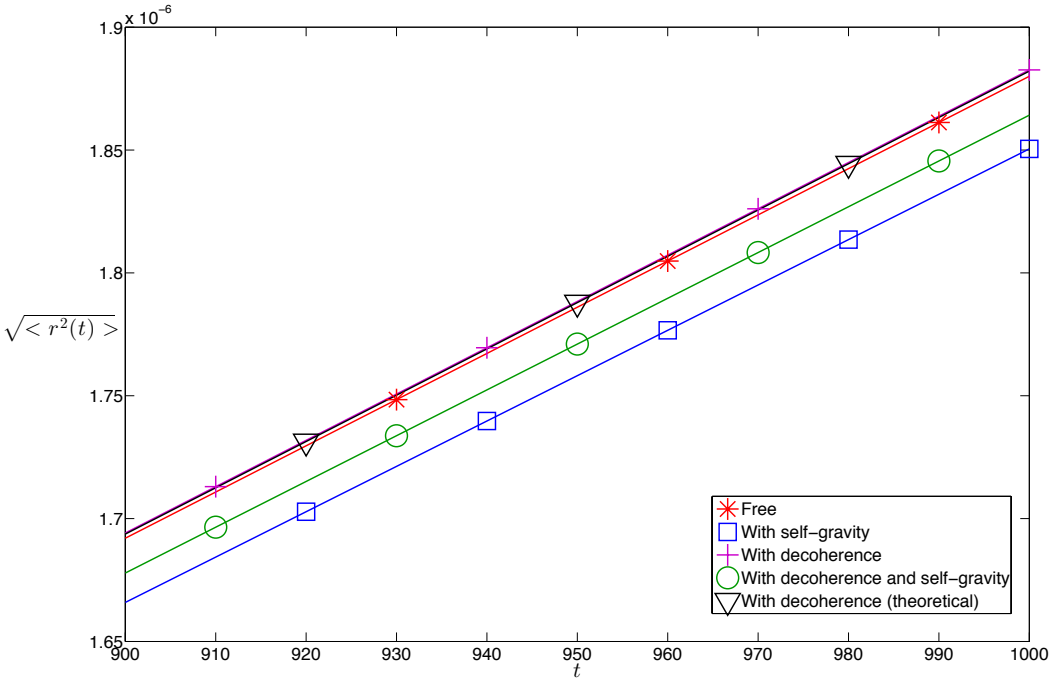

Figure 9: Spread (in m) of the CMDM for $t \in [900, 1000]$, for a nanosphere of radius 100 nm and mass density $\rho = 20000\,\mathrm{kg\,m^{-3}}$ (density of gold), with initial spread δr_0=10^{-9} m. The curves marked by squares and stars correspond to the absence of decoherence, respectively with and without self-gravity. The decoherence parameters are $\alpha = 10^{13}$ m^{-2} and $\gamma = 1$ s $^{-1}$. The curves marked by plus symbols and circles respectively correspond to the absence and presence of self-gravity, while the curve marked by triangles is the analytic curve (20).

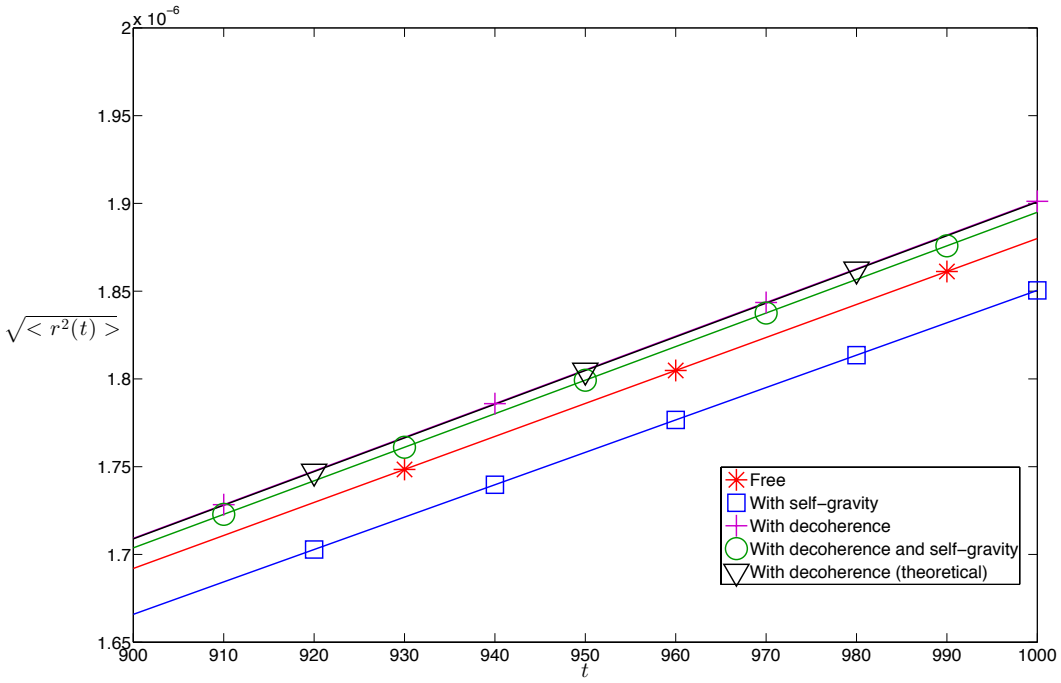

Figure 10: Spread (in m) of the CMDM for $t \in [900, 1000]$, for a nanosphere of radius 100 nm and mass density $\rho = 20000\,\mathrm{kg\,m^{-3}}$ (density of gold), with initial spread δr_0=10^{-9} m. The curves marked by squares and stars correspond to the absence of decoherence, respectively with and without self-gravity. The decoherence parameters are $\alpha = 10^{14}$ m^{-2} and $\gamma = 1$ s $^{-1}$. The curves marked by plus symbols and circles respectively correspond to the absence and presence of self-gravity, while the curve marked by triangles is the analytic curve (20).

(vi) As can be seen from figure 12 however, even if we limit ourselves to free falls with durations of 200 s, in case decoherence is low we can improve the situation by increasing the initial spread of the CMWF. In this case the influence of self-gravity is of the order of 20 nm after 200 s in the absence of decoherence (or when decoherence is negligible).

(vii) In the absence of any kind of exotic decoherence, provided the environmental decoherence is weak enough, self-gravity can still manifest itself even when the external decoherence is of the order of the critical parameter ($\Lambda \approx \Lambda_{crit}$). In this case, the optimal strategy would be (1) to make use of maximally dense spheres (say gold) in order to maximize self-gravity and (2) to prepare the initial state in the vicinity of the self-gravitationally bound state (which, in the cases represented in figures 7 to 14, can be estimated to be of the order of 10^{-8} m, on the basis of equation (11)). Indeed, as can be seen on figure 12, the effect of self-gravity is still clearly visible even in the presence of decoherence, provided decoherence is not too strong (the critical decoherence parameter value is estimated here, on the basis of equation (23), to be of the order of 10^{13}m^{-2} s^{-1}). Similar computations show that the effects are still present, though less pronounced, when the density is close to the normal density.

At this point, two important remarks regarding the feasibility of our experimental proposal impose themselves:

1. Each time a residual gas molecule gets scattered by the nanosphere, this will result in a contraction of the CMWF of the sphere to an extent ($\alpha^{-1/2}$) of the order of the angstroem. Even if this process does not occur very often, it can easily overwhelm the contributions of self-gravity and/or weak decoherence. This can be easily seen from equation (20), written in the form

$$< r^2 > (t) = \ < r^2 > (0) + \frac{9\hbar^2 t^2}{4M^2 < r^2 > (0)} + \frac{\Lambda \hbar^2 t^3}{2M^2}, \tag{27}$$

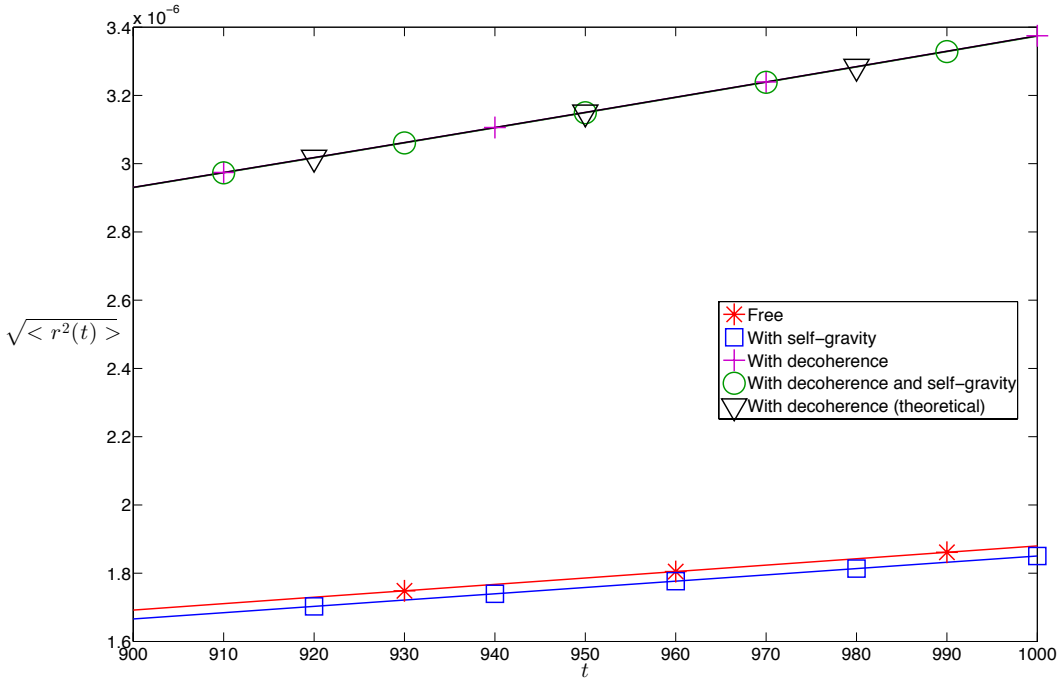

Figure 11: Spread (in m) of the CMDM for $t \in [900, 1000]$, for a nanosphere of radius 100 nm and mass density $\rho = 20000\,\mathrm{kg\,m^{-3}}$ (density of gold), with initial spread δr_0=10^{-9} m. The curves marked by squares and stars correspond to the absence of decoherence, respectively with and without self-gravity. The decoherence parameters are $\alpha = 10^{16}$ m^{-2} and $\gamma = 1$ s $^{-1}$. The curves marked by plus symbols and circles respectively correspond to the absence and presence of self-gravity, while the curve marked by triangles is the analytic curve (20).

where the contribution due to decoherence to the spread $< r^2 >$ is equal to $\Lambda\hbar^2t^3/2M^2$. For short times, after a collision, this contribution can be thought as the product of γt (i.e. the probability of a collision) with $\alpha\hbar^2t^2/2M^2$, which is the spread that we can attribute to the diffusion undergone by the free CMWF after the collision, i.e. corresponding to $< r^2 > (t = 0)=\alpha^{-2}$. In figure 14 (which is the only one in which the rate of jumps is the same as the rate of collisions with resiudal gas atoms or molecules: $\gamma = 4 \times 10^{-3}s^{-1}$) we see that the effects of environmental decoherence easily overwhelm the influence of gravitation, even when the number of collisions with gas molecules is low. Both influences may be dissociated experimentally however, provided they are separated by a post-selection process during which the population of nanospheres that have undergone a collision, gets separated from the population of nanospheres that did not. This is because of the fact that the spread of the first population explodes relative to the second population, as can be seen by comparing the change of scale between figures 13 and 14.

2. If we use optical traps to prepare the initial state of the CMWF, we are constrained by the size of the fundamental state in the trap which is of the order of 10^{-11} meter [32]. Nothing forbids us however to submit the nanosphere, either inside the trap or at the beginning of its free fall, to a well-suited environmental decoherence, for instance to a source of thermal photons, in order to modify the size of its individual CMWF according to our needs. For instance, making use of equation (19), it is easy to check that the equilibrium value $\delta r_{equil.} = (\hbar/M\Lambda)^{1/4}$ of a 100 nanometer radius gold nanosphere, is of the order of 100 nanometer too, provided that Λ is of the order of 10^{10} m^{-2} s^{-1}, which can be achieved by means of a source of black body photons at a temperature of the order of 50 kelvin. This preparation, which could be called *Planckian cooling*, exploits the frictious properties of decoherence in order to control the size of individual CMWF. Of course, it will result in some global loss of coherence [19, 50], but in our case coherence is not the most relevant parameter as we are not interested in realizing interference experiments.

In summary, we believe it is possible, for a limited range of parameters, to perform a crucial experiment aimed at checking whether the highly speculative equations (2–4) indeed capture the essence of self gravitational interaction in the mesoscopic regime. Thanks to our proposed device, it is also possible to explore a large set of exotic decoherence parameters, which have not been explored before [17] and which were unattainable in other proposals involving freely falling nanospheres based on measures of interference rather than on measures of the position spread[11].

7 Conclusions

Recent improvements of mechano-optical [4] and nano-optical [34, 31] devices nourish the hope that important and fundamental experiments will be realized in the near future, aimed at testing various non-standard proposals such as macro realist models and semi-classical self-gravitation models [2]. In this paper we proposed a new approach in which, instead of measuring the disappearance of interferences in the quantum-classical transition, crucial experiments are put forward based on the accurate measurement of the spread of freely falling nanospheres in a zero gravity environment. In order to correctly evaluate the temporal evolution of the spreading of their CMWF and CMDM, it was necessary to derive an exact expression for the self-interaction of the nanosphere in the mesoscopic regime (2) and to develop a numerical method based on the approximation scheme (5,9,10) which simplifies the resolution of the system (2–4), to such an extent that a Monte Carlo procedure mixing GRW jumps and gravitational-self focusing becomes computationally tractable.

In particular we showed, for the first time, that even in the presence of decoherence, self-gravitation gives rise to possibly observable effects, i.e.: that the self-gravitational influence is robust with respect to decoherence in a certain range of parameters[12]. Of course, these effects are small and in order to be able to observe the tiny influence of self-gravitation the experiment we propose must be realized in

[11] It is worth noting that remarks 1. and 2. concerning the need for a post-selection in position and a tailored preparation process using a well-controlled environmental source of decoherence, might also be of benefit to experiments that aim at measuring the survival of interferences in the mesoscopic regime.

[12] In [51] , van Meter wrote the following about the Schrödinger-Newton equation: *...this theory predicts significant deviation from conventional (linear) quantum mechanics. However, owing to the difficulty of controlling quantum coherence on the one hand, and the weakness of gravity on the other, definitive experimental falsification poses a technologically formidable challenge....*

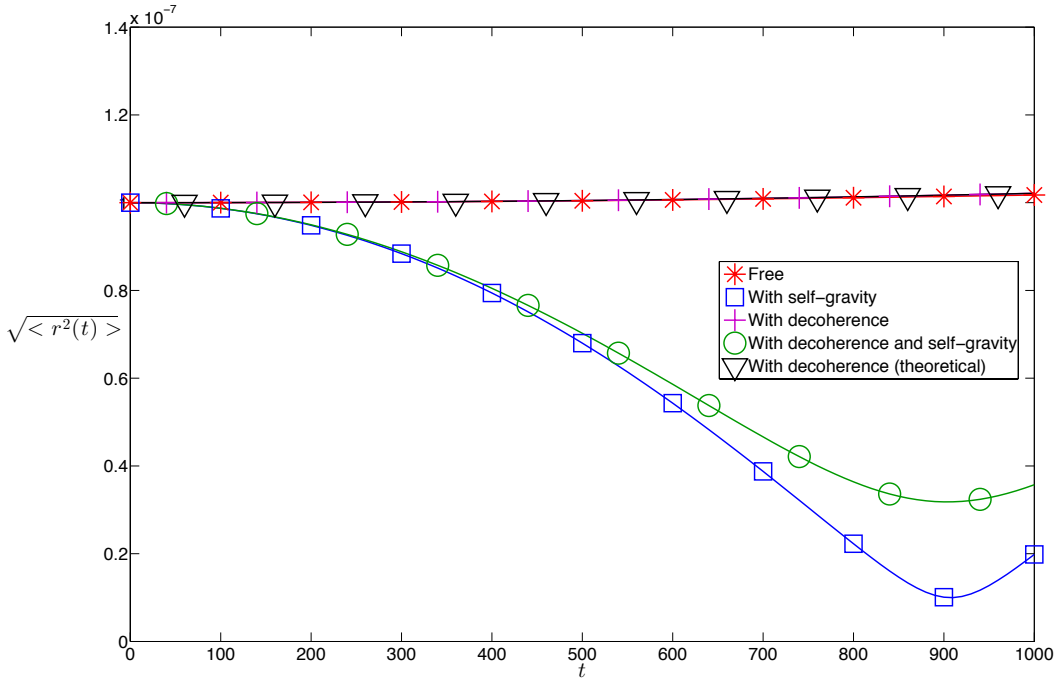

Figure 12: Spread (in m) of the CMDM for $t \in [0, 1000]$, for a nanosphere of radius 100 nm and mass density $\rho = 20000\,\mathrm{kg\,m^{-3}}$ (density of gold), with initial spread $\delta r_0{=}10^{-7}$ m. The curves marked by squares and stars correspond to the absence of decoherence, respectively with and without self-gravity. The decoherence parameters are $\alpha = 10^{11}$ m^{-2} and $\gamma = 1$ s $^{-1}$. The curves marked by plus symbols and circles respectively correspond to the absence and presence of self-gravity, while the curve marked by triangles is the analytic curve (20).

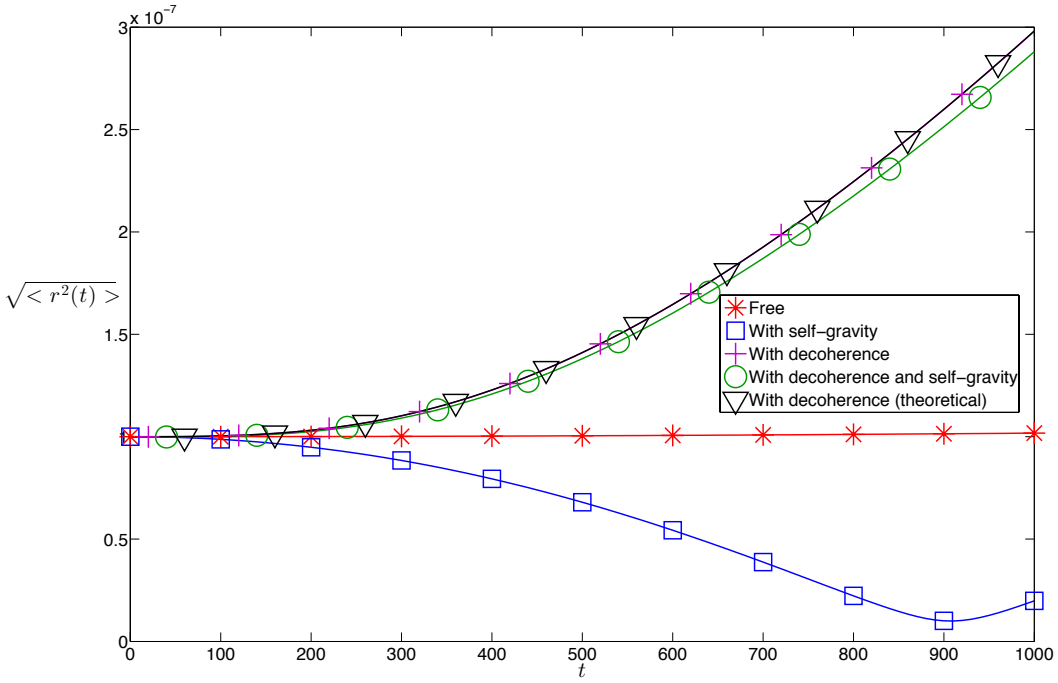

Figure 13: Spread (in m) of the CMDM for $t \in [0, 1000]$, for a nanosphere of radius 100 nm and mass density $\rho = 20000\,\mathrm{kg\,m^{-3}}$ (density of gold), with initial spread $\delta r_0{=}10^{-7}$ m. The curves marked by squares and stars correspond to the absence of decoherence, respectively with and without self-gravity. The decoherence parameters are $\alpha = 10^{14}$ m^{-2} and $\gamma = 1$ s^{-1}. The curves marked by plus symbols and circles respectively correspond to the absence and presence of self-gravity, while the curve marked by triangles is the analytic curve (20).

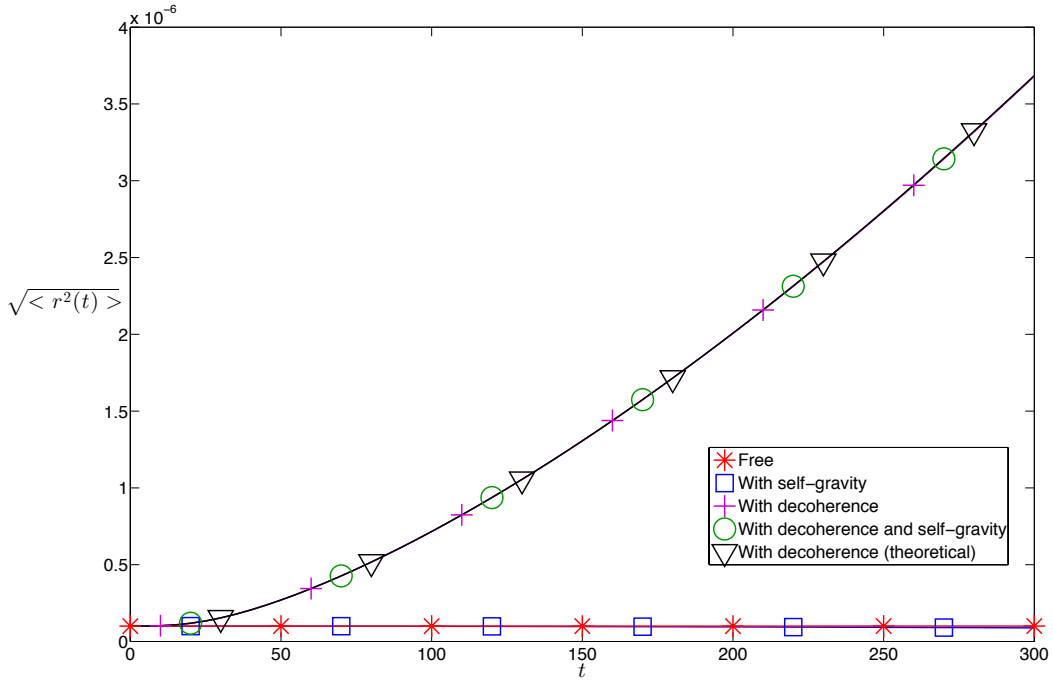

Figure 14: Spread (in m) of the CMDM for $t \in [0, 300]$, for a nanosphere of radius 100 nm and mass density $\rho = 20000\,\mathrm{kg\,m^{-3}}$ (density of gold), with initial spread $\delta r_0 = 10^{-7}$ m. The curves marked by squares and stars correspond to the absence of decoherence, respectively with and without self-gravity. The decoherence parameters are $\alpha = 1.6 \times 10^{20}$ m^{-2} and $\gamma = 4 \times 10^{-3}$ s^{-1}. The curves marked by plus symbols and circles respectively correspond to the absence and presence of self-gravity, while the curve marked by triangles is the analytic curve (20).

an extremely clean environment and will necessarily involve very accurate measurement techniques. In particular, measuring the spread in position of the nanosphere after its free fall requires one to go beyond the Abbe-Rayleigh limit.

Moreover, we demonstrated that the experimental set-up we propose, provides an alternative way to measure the physical manifestation of the hypothetical QG and CSL "strong" spontaneous localisation mechanisms, under conditions that are very similar to those required for interference experiments [33, 32, 42]. Our proposal therefore amounts to a crucial experiment aimed at testing whether these macro realist models grasp a deep aspect of reality and are indeed necessary for explaining the quantum classical transition. We also showed that, although difficult, it is not impossible to falsify the hypothetical DP "weak" spontaneous localisation mechanism in a similar fashion.

Finally, we provided a possible method to probe self-gravity in the case of weaker SL parameters for which self-gravity effects and decoherence effects are comparable (i.e., the case characterized by comparable values of Λ, cf. equations (16) and (24)), for which an interesting interplay appears between decoherence and self-gravity. It is obvious however that the original GRW parameters are far too weak to be possibly probed with our experimental set-up, but this holds true for all experiments that have been carried out so far with this aim [17].

Our proposal requires free fall times in the range 10^2 to 10^3 s, that are only possible in an inertial, freely falling frame (a satellite). We believe it would actually be one of the most interesting physics experiments, proposed so far, that requires the use of a satellite.

Acknowledgements

This work was made possible through the support of a grant from the John Templeton Foundation. TD and RW acknowledge support in the past from a mobility grant FWOKN184 "Solitonen en solitonachtige oplossingen van gedeeltelijk integreerbare niet-lineaire partieel differentiaalvergelijkingen met corpusculair gedrag". SC was supported by a PIAF fellowship (Perimeter Institute - Australia Foundations) for the period during which most of this research was conducted. The authors wish to express their gratitude to Professor Wiseman (Griffith University) for helpful comments on the manuscript, logistic and administrative support, and to Professor Lambert (Vrije Universiteit Brussel) for his encouragement during the initial phases of this project. One of us (TD) acknowledges fruitful discussions with A. Rahmani (University of Technology of Sydney), M. Guillaume, N. Bertaux (Phyti Institut Fresnel) , G. Maire, N. Sandeau (Semox Institut Fresnel), H, Ahmed, J. Savatier, H. Rigneault, G. Baffou (Mosaic Institut Fresnel), and with students and researchers of the ECM involved in the project Nanosatellite 2012-2013 as well as in the "Projet Transverse Freely Falling Microspheres in Satellite" 2013-2014 concerning technical issues like e.g. the possibility to use subwavelength techniques for measuring the positions of the nanospheres. He also thanks M. Aspelmeyer, for bringing to his attention recent developments in optomechanics and the possibility to trap and cool nanospheres by (quantum) optical methods, as well as his collaborators for enriching discussions on topics very close to those treated in the present paper (private discussions in Vienna, november 2012).

References

[1] S.L. Adler. *Quantum theory as an emergent phenomenon.* Cambridge University Press, Cambridge, 2004.

[2] A. Arndt, M.and Bassi, D. Giulini, A. Heidmann, and J-M Raimond. Fundamental frontiers of quantum science and technology. *Procedia Computer Science*, 7:77–80, 2011.

[3] E.R. Arriola and J. Soler. A Variational Approach to the Schrödinger-Poisson System: Asymptotic Behaviour, Breathers, and Stability. *J. Stat. Phys.*, 103(5-6):1069–1105, 2001.

[4] M. Aspelmeyer, P. Meystre, and K. Schwab. Quantum optomechanics. *Physics Today*, 65(7):29, 2012.

[5] A. Bassi, K. Lochan, S. Satin, T. P. Singh, and H. Ulbricht. Models of wave-function collapse, underlying theories, and experimental tests. *Rev. Mod. Phys.*, 85:471–527, 2013.

[6] J.S. Bell. Are there Quantum Jumps? In C.W. Kilmister, editor, *Schrödinger: Centenary celebration of a Polymath*, pages 172–192. Cambridge U.P., 1987.

[7] D.H. Bernstein, E. Giladi, and K.R.W. Jones. Eigenstates of the gravitational Schrödinger equation. *Mod. Phys. Lett. A*, 13(29):2327–2336, 1998.

[8] L. D. Carr, C. W. Clark, and W. P. Reinhardt. Stationary solutions of the one-dimensional nonlinear Schrödinger equation. II. Case of attractive nonlinearity. *Phys. Rev. A*, 62:063611, 2000.

[9] T. Cazenave and P.L. Lions. Orbital Stability of Standing Waves for Some Nonlinear Schrödinger Equations. *Commun. Math. Phys.*, 85:549, 1982.

[10] S. Colin, T. Durt, and R. Willox. Would a quantum particle succumb to its own gravitational attraction? arXiv:quant-ph/..., 2014.

[11] L. Diósi. Gravitation and quantum-mechanical localization of macro-objects. *Phys. Lett. A*, 105:199–202, 1984.

[12] L. Diósi. A universal master equation for the gravitational violation of the quantum mechanics. *Phys. Lett. A*, 120:377–381, 1987.

[13] L. Diósi. Models for universal reduction of macroscopic quantum fluctuations. *Phys. Rev. A*, 40:1165–1174, 1989.

[14] M. Ehrhardt and A. Zisowsky. Fast Calculation of Energy and Mass preserving solutions of Schrödinger-Poisson systems on unbounded domains. *Journal of Computational and Applied Mathematics*, 187:1–28, 2006.

[15] J. Ellis, N.E. Mavromatos, and D.V. Nanopoulos. String theory modifies quantum mechanics. *Phys. Lett. B.*, 37:37, 1992.

[16] J. Ellis, S. Mohanty, and D.V. Nanopoulos. Quantum gravity and the collapse of the wavefunction. *Phys. Lett. B.*, 221:113, 1989.

[17] W. Feldmann and R. Tumulka. Parameter Diagrams of the GRW and CSL Theories of Wave Function Collapse. *J. Phys. A*, 45:065304, 2012.

[18] A. Frenkel. Spontaneous localizations of the wave- function and classical behavior. *Found. Phys.*, 20(2):159–188, 1990.

[19] G.-C.Ghirardi, A. Rimini, and T. Weber. Unified dynamics for microscopic and macroscopic systems. *Phys. Rev. D*, 34(2):470–491, 1986.

[20] Gao, S. Does gravity induce wavefunction collapse? An examination of Penrose's argument. Online at http://philsci-archive.pitt.edu/8997/, 2012.

[21] S.J. Gerlich, S. Eibenberger, M. Tomandl, S. Nimmrichter, K. Hornberger, J. Tüxen, M. Mayor, and M. Arndt. Quantum interference of large organic molecules . *Nature Communications*, 2:263, 2012.

[22] G. Ghirardi, P. Pearle, and A. Rimini. Markov processes in hilbert space and continuous spontaneous localization of systems of identical particles. *Phys. Rev. A*, 42(1):78–89, 1990.

[23] D. Giulini and A. Großardt. Gravitationally induced inhibitions of dispersion according to the Schrödinger-Newton Equation. *Class. Quantum Grav.*, 28:195026, 2011.

[24] D. Giulini and A. Großardt. The Schrödinger-Newton equation as non-relativistic limit of self-gravitating Klein-Gordon and Dirac fields. *Class. Quantum Grav.*, 29:215010, 2012.

[25] F. S. Guzmán and L. A. Ureña López. Newtonian collapse of scalar field dark matter. *Phys. Rev. D*, 68:024023, 2003.

[26] F. S. Guzmán and L. A. Ureña López. Evolution of the Schrödinger-Newton system for a self-gravitating scalar field. *Phys. Rev. D*, 69:124033, 2004.

[27] S. Haroche and J.-M. Raimond. *Exploring the Quantum - Atoms, Cavities and Photons*. Oxford University Press, U.K., 2006.

[28] R. Harrison, I. Moroz, and K. P. Tod. A numerical study of the Schroedinger-Newton equations. *Nonlinearity*, 16:101–122, 2003.

[29] H. Iwe. Coulomb potentials between spherical heavy ions. *Z. Phys. A*, 304:347–361, 1982.

[30] E. Joos and H.D. Zeh. The emergence of classical properties through interaction with the environment. *Z. Phys. B: Condens Matter*, 59:223–243, 1985.

[31] T. Juffmann, A. Milic, M. Müllneritsch, P. Asenbaum, A. Tsukernik, J. Tüxen, M. Mayor, O. Cheshnovsky, and M. Arndt. Real-time single-molecule imaging of quantum interference. *Nature Nanotechnology*, 7:297–300, 2012.

[32] R. Kaltenbaek. Testing quantum physics in space using optically trapped nanospheres. arXiv:quant-ph/1307.7021, 2013.

[33] R. Kaltenbaek, G. Hechenblaikner, N. Kiesel, O. Romero-Isart, K.C. Schwab, U. Johann, and M. Aspelmeyer. Macroscopic quantum resonators (MAQRO). *Exp. Astron.*, 34(2):123–164, 2012. Online at http://arxiv.org/abs/1201.4756.

[34] Kim, H.J. and Selvin, P.R. Fluorescence Imaging with One Nanometer Accuracy. In GCK Roberts, editor, *Encyclopedia of Biophysics*, page 37. Springer, 2013.

[35] D. Kumar and V. Soni. Single particle Schrödinger equations with gravitational self-interaction. *Phys. Lett. A*, 271:157–166, 2000.

[36] E.H. Lieb. Existence and Uniqueness of the Minimizing Solution of Choquard's Nonlinear Equation. *Studies in Applied Mathematics*, 57:93–105, 1977.

[37] M. Membrado, A. F. Pacheco, and J. Sañudo. Hartree solutions for the self-Yukawian boson sphere. *Phys. Rev. A*, 39:4207–4211, 1989.

[38] C. Møller. The energy-momentum complex in general relativity and related problems. In A. Lichnerowicz and M.-A. Tonnelat, editor, *Les Théories Relativistes de la Gravitation - Colloques Internationaux CNRS 91*. CNRS, 1962.

[39] S. Nimmrichter, K. Hornberger, P. Haslinger, and M. Arndt. Testing spontaneous localization theories with matter-wave interferometry. *Phys. Rev. A*, 83:043621, 2011.

[40] P. Pearle. Combining stochastic dynamical state-vector reduction with spontaneous localization. *Phys. Rev. A*, 39(5):2277–2289, Mar 1989.

[41] R. Penrose. On Gravity's Role in Quantum State Reduction. *General Relativity and Gravitation*, 28(5):581–600, 1996.

[42] O. Romero-Isart. Quantum superposition of massive objects and collapse models. *Phys. Rev. A*, 84:052121, 2011.

[43] O. Romero-Isart, A. C. Pflanzer, F. Blaser, R. Kaltenbaek, N. Kiesel, M. Aspelmeyer, and J. I. Cirac. Large Quantum Superpositions and Interference of Massive Nanometer-Sized Objects. *Phys. Rev. Lett.*, 107:020405, Jul 2011.

[44] O. Romero-Isart, A. C. Pflanzer, M. L. Juan, R. Quidant, N. Kiesel, M. Aspelmeyer, and J. I. Cirac. Optically levitating dielectrics in the quantum regime: Theory and protocols. *Phys. Rev. A*, 83:013803, Jan 2011.

[45] L. Rosenfeld. On quantization of fields. *Nucl. Phys.*, 40:353–356, 1963.

[46] P.J. Salzman and S. Carlip. A possible experimental test of quantized gravity. arXiv:gr-qc/0606120, 2006.

[47] M. Schlosshauer. *Decoherence and the Quantum-to-Classical Transition.* Springer, Heidelberg Berlin, 2007.

[48] K.P. Tod. The ground state energy of the Schrödinger-Newton equation. *Phys. Lett. A*, 280:173–176, 2001.

[49] P. Tod and I. Moroz. An analytical approach to the Schrödinger-Newton equations. *Nonlinearity*, 12:201–216, 1999.

[50] B. Vacchini. On the precise connection between the GRW master-equation and master-equations for the description of decoherence. *J. Phys. A*, 40:2463–2473, 2007.

[51] J. R. van Meter. Schrödinger-Newton "collapse" of the wave-function. *Class. Quant. Grav.*, 28:215013, 2011.